National Library
of Canada

Acquisitions and
Bibliographic Services Branch

395 Wellington Street
Ottawa, Ontario
K1A 0N4

Bibliothèque nationale
du Canada

Direction des acquisitions et
des services bibliographiques

395, rue Wellington
Ottawa (Ontario)
K1A 0N4

Your file Votre référence

Our file Notre référence

NOTICE

The quality of this microform is heavily dependent upon the quality of the original thesis submitted for microfilming. Every effort has been made to ensure the highest quality of reproduction possible.

If pages are missing, contact the university which granted the degree.

Some pages may have indistinct print especially if the original pages were typed with a poor typewriter ribbon or if the university sent us an inferior photocopy.

Reproduction in full or in part of this microform is governed by the Canadian Copyright Act, R.S.C. 1970, c. C-30, and subsequent amendments.

AVIS

La qualité de cette microforme dépend grandement de la qualité de la thèse soumise au microfilmage. Nous avons tout fait pour assurer une qualité supérieure de reproduction.

S'il manque des pages, veuillez communiquer avec l'université qui a conféré le grade.

La qualité d'impression de certaines pages peut laisser à désirer, surtout si les pages originales ont été dactylographiées à l'aide d'un ruban usé ou si l'université nous a fait parvenir une photocopie de qualité inférieure.

La reproduction, même partielle, de cette microforme est soumise à la Loi canadienne sur le droit d'auteur, SRC 1970, c. C-30, et ses amendements subséquents.

Canada

University of Alberta

NONLINEAR ANALYSIS OF ROD DEFORMATIONS

By

DONALD WAYNE RABOUD

A thesis submitted to the Faculty of Graduate Studies and Research in partial fulfillment of the requirements for the degree of Master of Science.

Department of Mechanical Engineering

Fall 1992

National Library of Canada
Bibliothèque nationale du Canada

Canadian Theses Service
Service des thèses canadiennes

Ottawa, Canada
K1A 0N4

The author has granted an irrevocable non-exclusive licence allowing the National Library of Canada to reproduce, loan, distribute or sell copies of his/her thesis by any means and in any form or format, making this thesis available to interested persons.

L'auteur a accordé une licence irrévocable et non exclusive permettant à la Bibliothèque nationale du Canada de reproduire, prêter, distribuer ou vendre des copies de sa thèse de quelque manière et sous quelque forme que ce soit pour mettre des exemplaires de cette thèse à la disposition des personnes intéressées.

The author retains ownership of the copyright in his/her thesis. Neither the thesis nor substantial extracts from it may be printed or otherwise reproduced without his/her permission.

L'auteur conserve la propriété du droit d'auteur qui protège sa thèse. Ni la thèse ni des extraits substantiels de celle-ci ne doivent être imprimés ou autrement reproduits sans son autorisation.

ISBN 0-315-77307-3

Canada

University of Alberta

Release Form

Name of Author:	Donald Wayne Raboud
Title of Thesis:	Nonlinear Analysis of Rod Deformations
Degree:	Master of Science
Year This Degree Granted:	Fall 1992

Permission is hereby granted to the University of Alberta Library to reproduce single copies of this thesis and to lend or sell such copies for private, scholarly or scientific research purposes only.

The author reserves all other publication and other rights in association with the copyright in the thesis, and except as hereinbefore provided neither the thesis nor any substantial portion thereof may be printed or otherwise reproduced in any material form whatever without the author's prior written permission.

Donald W. Raboud

8619 - 94th avenue
Fort Saskatchewan, Alberta
T8L 2R7

Date: May 14, 1992

University of Alberta

Faculty of Graduate Studies and Research

The undersigned certify that they have read and recommend to the Faculty of Graduate Studies and Research for acceptance, a thesis entitled **Nonlinear Analysis of Rod Deformations** submitted by **Donald Wayne Raboud** in partial fulfillment of the requirements for the degree of **Master of Science**.

Gary Faulkner
Dr. M.G. Faulkner (Supervisor)

A W Lipsett
Dr. A.W. Lipsett (Co-supervisor)

David S Steigmann
Dr. D.J. Steigmann (Co-supervisor)

J R Colbourne.
Dr. J.R. Colbourne

T. Hrudey
Dr. T.M. Hrudey

Date: May 12, 1992

To Alina and my parents....

Abstract

The equations of equilibrium describing the large three dimensional deformations of rods are well established but due to their inherent nonlinearity are rarely directly solvable for practical problems.

In this thesis a numerical method, the *segmental shooting technique*, previously found to be useful for solving planar elastica problems is employed to analyse large three dimensional deformations of initially straight rods with circular cross sections. This method avoids the nonlinearity in the problem by considering the rod as a series of short segments. Each of these segments undergoes small relative deformations so that a linear solution can be individually applied over each segment. The total nonlinear solution is obtained by assembling a sequence of these linear solutions.

The technique was used to solve the problem of buckling of a rod by axial torsion and axial forces. This problem is one which exhibits multiple equilibrium solutions. The segmental technique was able to find these multiple solutions and was shown to compare favorably with the known analytical solutions.

Acknowledgements

I would like to take this opportunity to sincerely thank Dr. M.G. Faulkner, Dr. A.W. Lipsett and Dr. D.J. Steigmann for their valuable guidance and support throughout the course of this work. I also gratefully acknowledge NSERC for providing financial support through their scholarships and fellowships program.

I would also like to thank the following individuals for their help in various ways: Victor Tam, Raymond Mah, Jeffrey Kemps, Al Muir, Max Schubert and the Stability Support Group. My apologies to any person(s) I may have missed.

TABLE OF CONTENTS

		PAGE #
Chapter 1:	**Introduction**	1
	1.1: Background	2
	1.2: Thesis Outline	4
Chapter 2:	**Theoretical Development**	6
	2.1: Kinematics	7
	2.2: Potential Energy and Equilibrium	12
	2.3: Constitutive Relations	20
	2.4: Application of Equilibrium Equations - Helical Rod	23
Chapter 3:	**Segmental Shooting Technique**	28
	3.1: Equilibrium Equations For Small Deflections	29
	3.2: Power Series Solution	35
	3.2.1: Non-Dimensionalization	37
	3.2.2: Series Coefficients	41
	3.2.2: Forces, Deformations and Moments	42
	3.3: Solution Procedure	51
	3.4: Shooting Procedure	57
Chapter 4:	**Verification and Results**	60
	4.1: Helical Rod	61
	4.1.1: Helix With No Axial Forces	65
	4.1.2: Helix With Axial Forces	77
	4.2: Shooting Problem	85

TABLE OF CONTENTS (continued)

		Page #
Chapter 5:	**Conclusions**	90
	5.1: Summary	90
	5.2: Future Work	92
References		94

Appendices

Appendix A:	**Dimensional Analysis of Equilibrium Equation**	96
Appendix B:	**Alternate Bases at End of Segment**	104

LIST OF TABLES

		Page #
Table 4.1:	Geometry at the End of a Deformed Helix, M_z = 200 Nm, α = 45°	66
Table 4.2:	Overall Equilibrium of Solutions Obtained With Segmental Technique For an Increasing Number of Segments, M_z = 200 Nm, α = 45°	71
Table 4.3:	Geometry at the End of a Deformed Helix, M_z = 200 Nm, α = 75°	75
Table 4.4:	Overall Equilibrium of Solutions Obtained With Segmental Technique For an Increasing Number of Segments, M_z = 200 Nm, α = 75°	75
Table 4.5:	Overall Equilibrium of Solutions Obtained With Segmental Technique For an Increasing Number of Segments, M_z = 200 Nm, α = 5°	76
Table 4.6:	Convergence Behavior of One Variable Shooting Problem	89

LIST OF FIGURES

		Page #
Figure 2.1:	Straight Rod Deformed Into a Helix	24
Figure 3.1:	Small Deflection of Arbitrary Rod Segment	30
Figure 3.2:	Rod Segment	36
Figure 3.3:	Coordinates at End of Segment	46
Figure 4.1:	Straight Rod Deformed Into a Helix	61
Figure 4.2a:	Geometry of Deformed Helix - ZX Plane (500 Segments) M_z = 200 Nm, α = 45°	66
Figure 4.2b:	Geometry of Deformed Helix - ZY Plane (500 Segments) M_z = 200 Nm, α = 45°	67
Figure 4.2c:	Geometry of Deformed Helix - YX Plane (500 Segments) M_z = 200 Nm, α = 45°	67
Figure 4.3a:	Geometry of Deformed Helix - ZX Plane (20 Segments) M_z = 200 Nm, α = 45°	68
Figure 4.3b:	Geometry of Deformed Helix - ZY Plane (20 Segments) M_z = 200 Nm, α = 45°	69
Figure 4.3c:	Geometry of Deformed Helix - YX Plane (20 Segments) M_z = 200 Nm, α = 45°	69
Figure 4.4:	Twist Per Unit Length Along Rod (M_z = 200 Nm, α = 45°)	72
Figure 4.5:	Energy Integral Evaluated Along Rod (M_z = 200 Nm, α = 45°)	73
Figure 4.6a:	Geometry of Deformed Helix - ZX Plane (500 Segments) M_z = 200 Nm, F_z = 100 N, α = 45°, R = 0.0476961 m	79
Figure 4.6b:	Geometry of Deformed Helix - ZY Plane (500 Segments) M_z = 200 Nm, F_z = 100 N, α = 45°, R = 0.0476961 m	79
Figure 4.6c:	Geometry of Deformed Helix - YX Plane (500 Segments) M_z = 200 Nm, F_z = 100 N, α = 45°, R = 0.0476961 m	80

LIST OF FIGURES (continued)

		Page #
Figure 4.7:	Twist Per Unit Length Along Rod - (500 Segments) M_z = 200 Nm, F_z = 100 N, α = 45°, R = 0.0476961 m	81
Figure 4.8:	Energy Integral Evaluated Along Rod - (500 Segments) M_z = 200 Nm, F_z = 100 N, α = 45°, R = 0.0476961 m	81
Figure 4.9a:	Geometry of Deformed Helix - ZX Plane (500 Segments) M_z = 200 Nm, F_z = 100 N, α = 45°, R = 1.9523039 m	82
Figure 4.9b:	Geometry of Deformed Helix - ZY Plane (500 Segments) M_z = 200 Nm, F_z = 100 N, α = 45°, R = 1.9523039 m	83
Figure 4.9c:	Geometry of Deformed Helix - YX Plane (500 Segments) M_z = 200 Nm, F_z = 100 N, α = 45°, R = 1.9523039 m	83
Figure 4.10:	Twist Per Unit Length Along Rod - (500 Segments) M_z = 200 Nm, F_z = 100 N, α = 45°, R = 1.9523039 m	84
Figure 4.11:	Energy Integral Evaluated Along Rod - (500 Segments) M_z = 200 Nm, F_z = 100 N, α = 45°, R = 1.9523039 m	84
Figure 4.12:	Axial Length z as a Function of Initial Pitch Angle α	87

CHAPTER

ONE

INTRODUCTION

There are many structures of practical engineering importance which can be modelled as long slender rods that undergo large three dimensional deformations due to combined bending and twisting. A few examples are:

- Laying of pipeline in an offshore situation
- Orthodontic springs used to reposition teeth during orthodontic treatment
- Helical springs

It is important to be able to determine the forces and moments developed when these structures are deformed. The pipeline must be properly supported during installation or it may be damaged. The orthodontic springs must produce forces, moments and moment/force ratios within certain ranges in order to reposition teeth safely and effectively. Helical springs, such as those used in automotive suspension systems, are used in a wide variety of applications and often have complicated geometries (varying radius, pitch angle, cross section). The force/deflection response of the spring is of critical importance for many applications. Due to the inherently large three dimensional deflections which occur, however, the equations which govern the deformation are highly nonlinear and as such are difficult to solve analytically. This fact, coupled with the wide variety of boundary conditions to which such structures may be subjected, makes it

necessary to use numerical methods to solve the governing equations approximately. This thesis is concerned with the application of a numerical procedure, the *segmental shooting technique*, to this type of problem for the case where the rods under consideration are initially straight, inextensible and have a circular cross section.

1.1 BACKGROUND

The large deflections of rods have been the subject of research for some time due to the wide variety of practical applications as well as the fundamental nonlinearity of the problem. As a result, there is a vast amount of literature on the subject. It is not the purpose here to give a complete review of the pertinent literature but merely to give an indication of what is available.

The equations of equilibrium governing the three dimensional deformations of long slender rods are well known. In his treatise on elasticity, Love [1] presents a derivation of these equations based on that of Kirchhoff (1859). In this presentation, the more general case of a rod with two distinct principal axes in the cross section is assumed. As well extensibility is taken into account. The forces and moments are related to the components of the curvature and torsion of the centerline of the rod. Landau and Lifshitz [2] derive the equations of equilibrium of the rod based on an analysis of an arbitrary infinitesimal section of the rod. These equations were expressed in terms of the tangent vector and its derivative. Distributed forces were considered but distributed moments were not taken into account. Steigmann and Faulkner [3] obtained the equilibrium equations for a rod using variational calculus to minimize the potential energy of the deformed rod. The rod was considered to be a one dimensional continuum

with a strain energy which depends upon the bending and twisting along the rod. The equations obtained were identical to those of Landau and Lifshitz [2]. This work will be the starting point for what follows in the thesis.

Both Love [1] and Landau and Lifshitz [2] considered the problem of an initially straight rod with circular cross section twisted into a helix under the action of axial end moments and forces as an analytical application of the derived equations. This problem is discussed below in both Section 2.4 and Chapter 4 and represents one of a very limited number of analytical results which have been found for fully three dimensional problems.

Due to the difficulty of solving the complete three dimensional equations analytically, Surana and Sorem [4] have recently utilized a nonlinear finite element approach to model initially curved rods. An incremental loading technique, which greatly increases computational effort, was used to accommodate the large element rotations which can occur during the deformation.

For the planar case, a considerable number of solutions have been developed (see for example Frisch-Fay [5] and Wang [6]) as the geometry is simpler and there is no twisting of the cross section to consider. However, even in this case, the solutions available analytically are generally limited to those with uniform cross sections and subjected to very particular loading conditions. To allow a wider variety of problems to be effectively considered, a numerical method, known as the segmental shooting technique, has been developed. This technique avoids the nonlinearity in the problem by considering the rod as being made up of a large number of short segments each of which undergoes only small relative deflections. As a result the equations governing its

shape are linear and can be easily solved. Faulkner and Stredulinsky [7] first used this segmental technique to analyze problems including a tapered cantilever under distributed and concentrated loads as well as the stiffened catenary problem. The technique was later modified by El-Rayes [8] to include rods which were initially curved. He used the technique to analyze the large deflections of orthodontic springs which were modelled as a sequence of initially straight and curved rod sections [8],[9]. Faulkner et. al. [10] used the segmental shooting technique to investigate multiple equilibrium configurations for cantilevers and arches under a variety of loadings and boundary conditions. A partial stability analysis was also carried out, based on the minimum potential energy criterion, to determine the relative stability of each configuration. The purpose of this thesis is to extend this technique to three dimensional rod problems where the loads and deflections are not necessarily co-planar.

1.2 THESIS OUTLINE

Chapter 2 briefly summarizes the relevant portions of the work of Steigmann and Faulkner [3] due to its importance to the subsequent work. The equations of equilibrium are obtained and their application to the helix problem mentioned previously is presented. Some properties of the equilibrium equations are highlighted as they serve as accuracy checks for the numerical solutions obtained in Chapter 4.

Chapter 3 presents the application of the segmental shooting technique to fully three dimensional rod problems. The nonlinear equilibrium equations are simplified for the case where small deflections occur. A power series solution is then obtained for a short segment of the rod which undergoes small deflections. A method for assembling

rod segments maintaining continuity and compatibility is shown and the shooting procedure, used to ensure that boundary conditions are satisfied, is described.

Chapter 4 presents the results of the application of the numerical method developed in Chapter 3 to the helix problem described in Chapter 2 for problems in which shooting is not required. The problem is then modified to demonstrate the shooting procedure. Chapter 5 summarizes the results of the work and lists proposals for future research.

CHAPTER

TWO

THEORETICAL DEVELOPMENT

In this chapter, the kinematics, equations of equilibrium and the constitutive assumptions for rods are developed. While several authors have previously developed these equations [1] [2], this derivation closely follows the work done by Steigmann and Faulkner [3] since the subsequent linearization and series solution are based on this approach. A rod is defined to be a spatial curve (one-dimensional continuum) for which the modes of deformation are through bending and torsion as the rod is assumed to be inextensible. As well, following the Bernoulli-Euler hypotheses, under any deformation initially plane cross sections remain plane, experience no strain, and are everywhere normal to the space curve tangent. For the present work the case of initially straight, transversely isotropic rods will be investigated. The rod is said to be transversely isotropic in the sense that the properties of the cross section are independent of orientation (ie: any axis in the cross section is a principal axis).

A configuration of the rod is characterized by a set of co-ordinates and right-handed orthonormal bases, $\{\underline{r}(s), \underline{e}_i(s)\}$ respectively, which define the location and orientation at any point on the rod in terms of the arc length parameter s; $s \in [0,L]$. The vector $\underline{e}_1(s)$ is a unit vector in the tangent direction of increasing arc length. The vectors $\underline{e}_2(s)$ and $\underline{e}_3(s)$ are unit vectors embedded in the material which define the orientation of the cross section. In its initially undeformed configuration, $\{\underline{r}(s), \underline{e}_i(s)\}$ take on the values $\{\underline{x}(s), \underline{E}_i(s)\}$. This configuration will serve as a reference from which to measure

all kinematic variables. In particular, $\underline{x}(s) = \{x(s),0,0\}$ forms an initially straight rod aligned with a global $\underline{E}_1$ axis. The orthonormal basis $\{\underline{e}_i\}$ will sometimes be referred to as $\{\underline{t}, \underline{e}_\alpha\}$; α=2,3; to emphasize the important role played by $\underline{e}_1$ in the subsequent derivation.

2.1 KINEMATICS

In this section the kinematics of the deformation of the rod are investigated. Some restrictions on their allowable values are determined. As well, a tensorial measure of the deformation is obtained and used to develop some conditions in order to satisfy the requirement of strain energy invariance.

The tangent to the curve, $\underline{t}(s)$, is given by

$$\underline{t}(s) = \underline{r}'(s) \tag{2.1}$$

where the ′ notation indicates differentiation with respect to arc length s. This identifies $\underline{t}$ as a unit vector. Now since $\{\underline{e}_i\}$ and $\{\underline{E}_i\}$ are right-handed orthonormal bases it follows that any deformation from $\{\underline{E}_i\}$ to $\{\underline{e}_i\}$ must be a rotation, that is,

$$\underline{e}_i(s) = \underline{R}(s)\,\underline{E}_i(s)\,, \tag{2.2}$$

where $\underline{R}$ is a rotation given by $\underline{R} = \underline{e}_j \otimes \underline{E}_j$, ($\det\underline{R} = 1$, $\underline{R}^T = \underline{R}^{-1}$).

The rod is hypothesized to supply an elastic resistance to both changes in curvature of the centerline (bending) and relative twist between adjacent cross sections s and s+ds (twist). This twist should not be confused with the torsion of a curve used in differential geometry. The bending and twisting of the rod are measured by the functions $\underline{e}_i'(s)$. The tensor

$$\underline{G}(s) = \underline{e}_i' \otimes \underline{E}_i \tag{2.3}$$

accounts for that part of the rate of change of any embedded material vector that is due to changes in curvature and twist of the rod. Thus the rod is idealized as having a strain energy per unit arc length, $W(\underline{G};\underline{G}^\circ,s)$, where $\underline{G}^\circ$ is the value of $\underline{G}$ in the reference configuration. For the case of an initially straight rod ($\underline{E}_i$=constant), $\underline{G}^\circ = \underline{E}_i' \otimes \underline{E}_i = \underline{0}$. The explicit s-dependence is due to any non-uniformity of material properties which may be present. For the problems being considered it is assumed that there is no such dependence so the strain energy may be simply written as $W = W(\underline{G})$.

Since the $\{\underline{e}_i(s)\}$ are defined to form an orthonormal basis the following relations apply;

$$\underline{e}_i \cdot \underline{e}_j = \delta_{ij}, \tag{2.4a}$$

$$\underline{e}_i \cdot \underline{e}_j \times \underline{e}_k = e_{ijk}, \tag{2.4b}$$

$\forall s \in [0,L]$ where δ_{ij} is the Kronecker delta and e_{ijk} is the permutation symbol [11]. Differentiation of (2.4a) gives the result $\underline{e}_i' \cdot \underline{e}_j + \underline{e}_i \cdot \underline{e}_j' = 0$. Then defining $\Omega_{ij} = \underline{e}_i \cdot \underline{e}_j'$ gives

$$\Omega_{ij} = \underline{e}_i \cdot \underline{e}_j' = -\underline{e}_i' \cdot \underline{e}_j = -\Omega_{ji}, \tag{2.5}$$

which shows that the components Ω_{ij} are skew. It follows from (2.5) that $\underline{e}_i'$ can be written as

$$\begin{aligned} \underline{e}_i' &= \underline{W}\,\underline{e}_i, \\ \underline{W} &= \Omega_{jk}\,\underline{e}_j \otimes \underline{e}_k. \end{aligned} \tag{2.6}$$

From (2.5) and (2.6) it is apparent that $\underline{\mathbf{W}}$ is skew (ie: $\underline{\mathbf{W}}^T = -\underline{\mathbf{W}}$). From (2.2), (2.3) and (2.6) it follows that $\underline{\mathbf{G}}\,\underline{\mathbf{E}}_i = \underline{\mathbf{W}}\,\underline{\mathbf{R}}\,\underline{\mathbf{E}}_i$ and since $\{\underline{\mathbf{E}}_i\}$ is an orthonormal basis this gives the result

$$\underline{\mathbf{G}} = \underline{\mathbf{W}}\,\underline{\mathbf{R}}, \quad \underline{\mathbf{W}} = \underline{\mathbf{G}}\,\underline{\mathbf{R}}^T = \underline{\mathbf{e}}_i' \otimes \underline{\mathbf{e}}_i. \tag{2.7}$$

A requirement of the strain energy is that it be unaffected by superimposed rigid body rotations. These arbitrary rotations are represented by $\underline{\mathbf{Q}}$, a constant rotation tensor. Under such a rotation the kinematic variables become

$$\begin{aligned} \underline{\mathbf{e}}_i^* &= \underline{\mathbf{Q}}\,\underline{\mathbf{e}}_i, \\ \underline{\mathbf{R}}^* &= \underline{\mathbf{Q}}\,\underline{\mathbf{R}}, \\ (\underline{\mathbf{e}}_i^*)' &= (\underline{\mathbf{Q}}\,\underline{\mathbf{e}}_i)' = \underline{\mathbf{Q}}\,\underline{\mathbf{e}}_i', \\ \underline{\mathbf{G}}^* &= (\underline{\mathbf{e}}_i^*)' \otimes \underline{\mathbf{E}}_i = \underline{\mathbf{Q}}(\underline{\mathbf{e}}_i' \otimes \underline{\mathbf{E}}_i) = \underline{\mathbf{Q}}\,\underline{\mathbf{G}}, \end{aligned} \tag{2.8}$$

where the * superscript indicates that the variable is under the influence of the arbitrary rotation. As a result, the invariance of strain energy requires that $W(\underline{\mathbf{G}})=W(\underline{\mathbf{Q}}\,\underline{\mathbf{G}})$ for all constant rotations $\underline{\mathbf{Q}}$, or using (2.7) this becomes

$$W(\underline{\mathbf{G}}) = W(\underline{\mathbf{W}}\,\underline{\mathbf{R}}) = W(\underline{\mathbf{Q}}\,\underline{\mathbf{W}}\,\underline{\mathbf{R}}). \tag{2.9}$$

To obtain a necessary condition for (2.9) to be valid, $\underline{\mathbf{Q}}$ is chosen to be the rotation $\underline{\mathbf{R}}^T$. Then (2.9) gives

$$W(\underline{\mathbf{G}}) = W(\underline{\mathbf{R}}^T\underline{\mathbf{W}}\,\underline{\mathbf{R}}) = W(\underline{\Omega}), \tag{2.10}$$

where $\underline{\Omega}$ is defined as

$$\underline{\Omega} = \underline{\mathbf{R}}^T\underline{\mathbf{W}}\,\underline{\mathbf{R}}. \tag{2.11}$$

Recalling (2.7) gives

$$\underline{\Omega} = \underline{R}^T(\Omega_{ij}\underline{e}_i\otimes\underline{e}_j)\underline{R} = \Omega_{ij}(\underline{R}^T\underline{e}_i\otimes\underline{R}^T\underline{e}_j) = \Omega_{ij}\underline{E}_i\otimes\underline{E}_j. \tag{2.12}$$

Comparing (2.6) and (2.12) shows that a necessary condition is that the components of $\underline{\Omega}$ relative to the reference basis $\{\underline{E}_i\}$ are the same as those of $\underline{W}$ relative to the deformed basis $\{\underline{e}_i\}$. Also, from (2.5) $\underline{\Omega}$ is shown to be skew.

To obtain a sufficient condition for invariance of strain energy note that for an arbitrary constant rotation $\underline{Q}$; $\underline{G}^* = \underline{Q}\,\underline{G}$ and $\underline{R}^* = \underline{Q}\,\underline{R}$. Thus $\underline{\Omega}^*$ is given by

$$\underline{\Omega}^* = (\underline{R}^*)^T\underline{G}^* = (\underline{Q}\,\underline{R})^T(\underline{Q}\,\underline{G}) = \underline{R}^T\underline{Q}^T\underline{Q}\,\underline{G} = \underline{R}^T\underline{G} = \underline{\Omega}, \tag{2.13}$$

or $\underline{\Omega}^* = \underline{\Omega}$. Thus $W(\underline{G}^*)=W(\underline{\Omega}^*)=W(\underline{\Omega})=W(\underline{G})$ for all constant rotations $\underline{Q}$. Therefore the invariance of the strain energy expressed in equation (2.9) is satisfied if and only if

$$\begin{gathered} W(\underline{G}) = W(\underline{\Omega}), \\ \underline{\Omega} = \Omega_{ij}\underline{E}_i\otimes\underline{E}_j, \quad \Omega_{ij} = \underline{e}_i\cdot\underline{e}'_j. \end{gathered} \tag{2.14}$$

The skew tensor $\underline{\Omega}$ is equivalent to its axial vector $\underline{\kappa}$ ($\underline{\kappa} = \kappa_i\,\underline{E}_i$) in the sense that $\underline{\Omega}\,\underline{u} = \underline{\kappa}\times\underline{u}$ for all vectors $\underline{u}$. More specifically, there are the identities [11]

$$\kappa_i = \tfrac{1}{2}e_{ijk}\Omega_{kj}, \quad \Omega_{kj} = \kappa_i e_{ijk}, \tag{2.15}$$

which relate the components of $\underline{\Omega}$ and $\underline{\kappa}$. As a result of this equivalence the strain energy can be functionally expressed as being dependent upon the vector $\underline{\kappa}$, ie;

$$W(\underline{\Omega}) = w(\underline{\kappa}). \tag{2.16}$$

In what follows both W and w are assumed to be twice differentiable over their domain of definition.

Equations (2.5) and (2.15) show that the components of $\underline{\kappa}$ are dependent upon the vectors $\underline{e}_i$ and $\underline{e}_i'$. Therefore the strain energy can be expressed as being a function, U, of $\underline{e}_i$ and $\underline{e}_i'$,

$$W(\underline{G}) = W(\underline{\Omega}) = w(\underline{\kappa}) = U(\underline{e}_i, \underline{e}_i'). \tag{2.17}$$

With the strain energy expressed in this form the requirement of invariance needs to be re-examined to determine its consequences. Following a similar procedure as before, the invariance of strain energy requires that

$$U(\underline{e}_i, \underline{e}_i') = U(\underline{Q}\,\underline{e}_i, \underline{Q}\,\underline{e}_i') \tag{2.18}$$

for all constant rotations $\underline{Q}$. To obtain a necessary condition for (2.18) consider the family of one-parameter constant rotations

$$\underline{Q}(\epsilon) = \exp(\epsilon \underline{V}) = \underline{I} + \sum_{n=1}^{\infty} \left(\frac{\epsilon^n}{n!} \right) \underline{V}^n, \tag{2.19}$$

where $\underline{V}$ is a constant skew tensor and $\underline{I}$ is the unit tensor. If $\underline{v}$ is defined to be the axial vector of $\underline{V}$ then for small ϵ,

$$\underline{Q}\,\underline{e}_i = \underline{e}_i + \epsilon \underline{v} \times \underline{e}_i + o(\epsilon), \quad \underline{Q}\,\underline{e}_i' = \underline{e}_i' + \epsilon \underline{v} \times \underline{e}_i' + o(\epsilon), \tag{2.20}$$

where $o(\epsilon)$ indicates terms which approach zero faster than ϵ as $\epsilon \to 0$. Using a Taylor series to expand the right-hand side of (2.18) about $\underline{e}_i$ and $\underline{e}_i'$ gives

$$U(\underline{Q}\,\underline{e}_i, \underline{Q}\,\underline{e}_i') = U(\underline{e}_i, \underline{e}_i') + \frac{\partial U}{\partial \underline{e}_i} \cdot (\epsilon \underline{v} \times \underline{e}_i) + \frac{\partial U}{\partial \underline{e}_i'} \cdot (\epsilon \underline{v} \times \underline{e}_i') + o(\epsilon), \tag{2.21}$$

where the convention is used that for a scalar valued function of vectors ($F(\underline{a},\underline{b})$), the derivatives $\partial F/\partial \underline{a}$ and $\partial F/\partial \underline{b}$ are defined to be $(\partial F/\partial a_i)\underline{c}_i$ and $(\partial F/\partial b_i)\underline{c}_i$ respectively where $\{\underline{c}_i\}$ is an arbitrary orthonormal basis and $\underline{a} = a_i\ \underline{c}_i$, $\underline{b} = b_i\ \underline{c}_i$. Combining (2.18) and (2.21) gives

$$\epsilon\left(\underline{v}\times\underline{e}_i\cdot\frac{\partial U}{\partial \underline{e}_i} + \underline{v}\times\underline{e}'_i\cdot\frac{\partial U}{\partial \underline{e}'_i}\right) + o(\epsilon) = 0. \tag{2.22}$$

Dividing (2.22) by ϵ, then letting $\epsilon \to 0$ and using the vector property $\underline{a}\times\underline{b}\cdot\underline{c} = \underline{a}\cdot\underline{b}\times\underline{c}$ gives the result

$$\underline{v}\cdot\left(\underline{e}_i\times\frac{\partial U}{\partial \underline{e}_i} + \underline{e}'_i\times\frac{\partial U}{\partial \underline{e}'_i}\right) = 0. \tag{2.23}$$

Since $\underline{v}$ is arbitrary, the condition of strain energy invariance expressed in equation (2.18) requires that, as a necessary condition,

$$\underline{e}_i\times\frac{\partial U}{\partial \underline{e}_i} + \underline{e}'_i\times\frac{\partial U}{\partial \underline{e}'_i} = \underline{0}. \tag{2.24}$$

This result will be useful later.

2.2 POTENTIAL ENERGY AND EQUILIBRIUM

In this section equilibrium equations for the rod are developed by using a variational procedure to obtain configurations of the rod which cause the potential energy to be stationary. Since a potential energy function is used, only conservative loads are considered here. A simple example is presented to show the essential steps in the

derivation.

The restrictions on the kinematics developed in the previous section introduce constraints which complicate the variational procedure. To accommodate this problem, a general expression is developed which satisfies these kinematic restrictions. This expression is used to remove the constraints and thus simplify the variational problem.

For a conservative system, an equilibrium position is defined as a configuration of the rod for which the potential energy, E( ), is stationary (ie: gradient of the potential energy function is zero). For the rod problem being considered, the potential energy is of the form

$$E(\underline{r},\underline{e}_i) = S(\underline{e}_i) - P(\underline{r},\underline{e}_i), \tag{2.25}$$

where

$$S(\underline{e}_i) = \int_0^L U(\underline{e}_i,\underline{e}_i')\,ds \tag{2.26}$$

is the total strain energy of the deformed rod and $P(\underline{r}, \underline{e}_i)$ is the load potential associated with a system of conservative loads.

For the purpose of illustration, the only loads to be considered will be a dead force $\underline{f}$ applied at the end s=L and a dead distributed load $\underline{b}(s)$ per unit length of the rod which is assumed to be at least piecewise continuous. These dead loads are conservative since the potential energies associated with them depend only upon the deformed configuration of the rod and are not path dependent. A further kinematical assumption is that $\underline{r}(0)$ and $\underline{e}_i(0)$ are specified and that the end s=L is free. With this class of loading the load potential becomes

$$P(\underline{r}) = \int_0^L (\underline{b}\cdot\underline{r})\,ds + \underline{f}\cdot\underline{r}(L), \tag{2.27}$$

which is a function of $\underline{r}$ only (independent of $\{\underline{e}_i\}$). For these loads equation (2.25) becomes

$$E(\underline{r},\underline{e}_i) = \int_0^L \left[U(\underline{e}_i,\underline{e}_i') - \underline{b}\cdot\underline{r} \right] ds - \underline{f}\cdot\underline{r}(L). \tag{2.28}$$

To obtain the equilibrium equations and natural boundary conditions, the first variation of the potential energy is used with a suitable class of kinematically admissable displacement fields. For the problem being considered the perturbations are

$$\underline{r}^* = \underline{r}(s) + \epsilon\underline{u}(s) + o(\epsilon), \tag{2.29a}$$

$$\underline{e}_i^* = \underline{e}_i(s) + \epsilon\underline{v}_i(s) + o(\epsilon), \tag{2.29b}$$

where the * superscript indicates values corresponding to the perturbed configuration. Here and $\underline{u}$ and $\underline{v}_i$ are the kinematically admissible displacement fields corresponding to the position $\underline{r}$ and the material basis $\underline{e}_i$ respectively. The displacement fields used in this case are not arbitrary but are subject to the constraint expressed in equation (2.4) that the vectors $\{\underline{e}_i^*(s)\}$ are orthonormal. Combining equations (2.4a) and (2.29b) gives the result

$$\delta_{ij} = \underline{e}_i^*\cdot\underline{e}_j^* = \delta_{ij} + \epsilon\left(\underline{e}_i\cdot\underline{v}_j + \underline{e}_j\cdot\underline{v}_j\right) + o(\epsilon). \tag{2.30}$$

Dividing (2.30) by ϵ ϵ and then letting $\epsilon\to 0$ gives

$$\underline{e}_i\cdot\underline{v}_j + \underline{e}_j\cdot\underline{v}_i = 0. \tag{2.31}$$

This is a restriction on the admissible values which $\underline{v}_i$ are allowed to assume. To obtain a general solution to (2.31) note that there is a tensor $\underline{\alpha}$ such that

$$\underline{v}_i = \underline{\alpha}\,\underline{e}_i, \tag{2.32}$$

where

$$\underline{\alpha} = \alpha_{ij}\,\underline{e}_i \otimes \underline{e}_j, \tag{2.33a}$$

$$\alpha_{ij} = \underline{e}_i \cdot \underline{v}_j. \tag{2.33b}$$

From (2.33b) and (2.31) it follows that $\alpha_{ij} = -\alpha_{ji}$ so that $\underline{\alpha}$ is skew. Consequently, there is a vector $\underline{a}$, the axial vector of $\underline{\alpha}$, such that

$$\underline{v}_i = \underline{a} \times \underline{e}_i. \tag{2.34}$$

Substituting (2.34) into (2.31) gives

$$\underline{e}_i \cdot \underline{a} \times \underline{e}_j + \underline{e}_j \cdot \underline{a} \times \underline{e}_i = \underline{a} \cdot \left(\underline{e}_i \times \underline{e}_j + \underline{e}_j \times \underline{e}_i\right), \tag{2.35}$$

which vanishes identically. Thus equation (2.34) is the general solution of the constraint equation given by (2.31) which is the variational version of the constraint given in (2.4a). With $\underline{v}_i$ given by (2.34) it is easily shown that variational version of the constraint expressed in (2.4b) is also identically satisfied. For future reference, combining (2.34) with (2.29b) for i=1 gives

$$\underline{e}_1^* = \underline{t}^* = \underline{t} + \epsilon\,\underline{a} \times \underline{t} + o(\epsilon). \tag{2.36}$$

Taking the first derivative of (2.36) with respect to ϵ and letting $\epsilon \to 0$ yields

$$\frac{d}{d\epsilon}\underline{t}^* = \underline{a} \times \underline{t}. \tag{2.37}$$

Recalling from equation (2.1) that $\underline{t}=\underline{r}'$, combining with (2.29a), taking the derivative with respect to ε and again letting $\varepsilon \to 0$ gives

$$\frac{d}{d\varepsilon}\underline{t}^* = \frac{d}{d\varepsilon}\underline{r}^{*\prime} = \frac{d}{d\varepsilon}(\underline{t}+\varepsilon\underline{u}'+o(\varepsilon)) = \underline{u}'. \tag{2.38}$$

Finally, comparing (2.37) and (2.38) gives the desired result

$$\underline{u}' = \underline{a}\times\underline{t}. \tag{2.39}$$

This will be useful later in determining the equations of equilibrium from the principles of the calculus of variations.

According to the multiplier rule of the calculus of variations [12], an admissible configuration that renders $E(\underline{r},\underline{e}_i)$ stationary is also a stationary configuration of the functional $\hat{E}(\underline{r},\underline{e}_i)$, where

$$\hat{E}(\underline{r},\underline{e}_i) = E(\underline{r},\underline{e}_i) + \int_0^L \underline{F}\cdot(\underline{r}'-\underline{t})\,ds \tag{2.40}$$

and $\underline{F}$ is a vector of Lagrange multipliers. For the case of (2.29) where $\{\underline{r},\underline{e}_i\}$ and $\{\underline{u},\underline{v}_i\}$ are independent of ε the functional $\hat{E}(\underline{r}^*,\underline{e}_i^*)$ is a function of one parameter (ε), that is

$$F(\varepsilon) = \hat{E}(\underline{r}^*,\underline{e}_i^*). \tag{2.41}$$

Then for a stationary potential energy (corresponding to an equilibrium position) it is required that $(dF/d\varepsilon)_{\varepsilon=0} = 0$ where, recalling (2.28),

$$\frac{dF}{d\epsilon}\Big|_{\epsilon=0} = -\int_0^L \left[\frac{\partial U}{\partial \underline{e}_i} \cdot \frac{\partial \underline{e}_i}{\partial \epsilon} + \frac{\partial U}{\partial \underline{e}_i'} \cdot \frac{\partial \underline{e}_i'}{\partial \epsilon} - \underline{b} \cdot \frac{\partial \underline{r}}{\partial \epsilon} + F \cdot \frac{\partial}{\partial \epsilon}(\underline{r}' - \underline{t}) \right] ds \tag{2.42}$$

$$- f \cdot \frac{\partial \underline{r}(L)}{\partial \epsilon} .$$

Using (2.29) and (2.39) this becomes

$$\frac{dF}{d\epsilon}\Big|_{\epsilon=0} = -\int_0^L \left[\underline{v}_i \cdot \frac{\partial U}{\partial \underline{e}_i} + \underline{v}_i' \cdot \frac{\partial U}{\partial \underline{e}_i'} - \underline{b} \cdot \underline{u} + F \cdot (\underline{u}' - \underline{a} \times \underline{t}) \right] ds \tag{2.43}$$

$$- f \cdot \underline{u}(L),$$

where the derivatives of U are evaluated at $\epsilon = 0$.

After integrating (2.43) by parts, using (2.34), recalling that $\{\underline{r}(0), \underline{e}_i(0)\}$ are fixed and that the end s=L is free, and further using the following definition,

$$M = \underline{e}_i \times \frac{\partial U}{\partial \underline{e}_i'}, \tag{2.44}$$

equation (2.43) simplifies to

$$\frac{dF}{d\epsilon}\Big|_{\epsilon=0} = \underline{a}(L) \cdot M(L) + \underline{u}(L) \cdot [F(L) - f]$$

$$-\int_0^L \underline{a} \cdot \left[M' - \left(\underline{e}_i \times \frac{\partial U}{\partial \underline{e}_i} + \underline{e}_i' \times \frac{\partial U}{\partial \underline{e}_i'} \right) - F \times \underline{t} \right] ds \tag{2.45}$$

$$-\int_0^L \underline{u} \cdot [F' + \underline{b}] ds .$$

Therefore, invoking the fundamental lemma of the calculus of variations, the configuration $\{\underline{r},\underline{e}_i\}$ renders the potential energy $E(\underline{r},\underline{e}_i)$ stationary if and only if the natural boundary conditions

$$\underline{M}(L) = \underline{0}, \tag{2.46a}$$

$$\underline{F}(L) = \underline{f}, \tag{2.46b}$$

are met and the Euler-Lagrange equations

$$\underline{F}\times\underline{t} = \underline{M}' - \left(\underline{e}_i \times \frac{\partial U}{\partial \underline{e}_i} + \underline{e}'_i \times \frac{\partial U}{\partial \underline{e}'_i}\right), \tag{2.47}$$

$$\underline{F}' + \underline{b} = \underline{0}, \tag{2.48}$$

are satisfied. Using the requirement of invariant strain energies expressed in (2.24), (2.47) simplifies to

$$\underline{F}\times\underline{t} = \underline{M}'. \tag{2.49}$$

This equation identifies $\underline{M}$ as a moment, where $\underline{M}$ is defined by (2.44). Equation (2.46b) identifies $\underline{F}(L)$ as the force applied at the end of the rod by an external source. Similarly, (2.46a) gives that the moment at the end of the rod must be zero, as expected. Equations (2.48) and (2.49) show that $\underline{F}$ and $\underline{M}$ are the force and moment, respectively, that act upon the material in the part [0,s] due to material in the part (s,L] of the rod. Hence (2.48) and (2.49) are the classical equilibrium equations of rod theory.

The previous results can be used to obtain a generalization of the classical *energy integral* [1] which will be useful in subsequent portions of this thesis. To start with, taking the first derivative of the strain energy, expressed in (2.17) as $U(\underline{e}_i,\underline{e}_i')$, with

respect to arc length yields

$$U' = \underline{e}_i' \cdot \frac{\partial U}{\partial \underline{e}_i} + \underline{e}_i'' \cdot \frac{\partial U}{\partial \underline{e}_i'}. \tag{2.50}$$

Recall from (2.6) that $\underline{e}_i' = \underline{W}\,\underline{e}_i$ where $\underline{W} = \Omega_{ij}\,\underline{e}_i \otimes \underline{e}_j$. Since $\underline{W}$ is skew it is equivalent to its axial vector $\underline{w}$ in the sense that

$$\underline{e}_i' = \underline{W}\,\underline{e}_i = \underline{w} \times \underline{e}_i. \tag{2.51}$$

The components of $\underline{w}$ are given by

$$w_i = \tfrac{1}{2} e_{ijk} \Omega_{kj}, \quad \Omega_{kj} = \underline{e}_k \cdot \underline{e}_j'. \tag{2.52}$$

These are the same as the components of $\underline{\kappa}$ (but with respect to a different basis) as given in (2.15). Differentiating (2.51) with respect to arc length and substituting into (2.50) gives

$$U' = \underline{w} \times \underline{e}_i \cdot \frac{\partial U}{\partial \underline{e}_i} + \underline{w} \times \underline{e}_i' \cdot \frac{\partial U}{\partial \underline{e}_i'} + \underline{w}' \times \underline{e}_i \cdot \frac{\partial U}{\partial \underline{e}_i'}. \tag{2.53}$$

Using the definition in (2.44) this becomes

$$U' = \underline{w} \cdot \left(\underline{e}_i \times \frac{\partial U}{\partial \underline{e}_i} + \underline{e}_i' \times \frac{\partial U}{\partial \underline{e}_i'} \right) + \underline{w}' \cdot \underline{M}, \tag{2.54}$$

where the first term on the right is zero because of the invariance requirement expressed in equation (2.24). The remaining term can be expressed as

$$U' = \underline{w}' \cdot \underline{M} = (\underline{w} \cdot \underline{M})' - \underline{w} \cdot \underline{M}'. \tag{2.55}$$

The last term of (2.55) becomes, using (2.49),

$$-\underline{w}\cdot\underline{M}' = -\underline{w}\cdot\underline{F}\times\underline{t} = \underline{F}\cdot\underline{w}\times\underline{t}. \tag{2.56}$$

But substituting (2.51) with i=1 into (2.56) gives

$$\underline{F}\cdot\underline{w}\times\underline{t} = \underline{F}\cdot\underline{t}' = (\underline{F}\cdot\underline{t})' - \underline{F}'\cdot\underline{t}. \tag{2.57}$$

Using equation (2.48), the last term in (2.57) becomes

$$-\underline{F}'\cdot\underline{t} = \underline{b}\cdot\underline{t}. \tag{2.58}$$

Substituting (2.55), (2.56), (2.57) and (2.58) into (2.54) gives the result

$$(U - \underline{w}\cdot\underline{M} - \underline{F}\cdot\underline{t})' = \underline{b}\cdot\underline{t}. \tag{2.59}$$

For the important case where $\underline{b}$ = constant, (2.59) results in a first integral

$$U - \underline{w}\cdot\underline{M} - \underline{F}\cdot\underline{t} - \underline{b}\cdot\underline{r} = \text{const.} \tag{2.60}$$

This pointwise expression for the energy will serve as a necessary condition which must be satisfied by any solution obtained using the numerical method developed in subsequent chapters.

2.3 CONSTITUTIVE RELATIONS

The rods considered in this thesis are assumed to have a quadratic strain energy function given by

$$W(\kappa) = \frac{1}{2} EI(\kappa_2^2 + \kappa_3^2) + \frac{1}{2} GJ\kappa_1^2 = U(\underline{e}_i, \underline{e}_i'), \tag{2.61}$$

where the κ_i terms are given by equation (2.15). To obtain an expression for the moment, defined by (2.44), the term $(\partial U/\partial \underline{e}_i')$ becomes

$$\frac{\partial U}{\partial \underline{e}_i'} = \frac{\partial W}{\partial \kappa_j}\frac{\partial \kappa_j}{\partial \underline{e}_i'}. \tag{2.62}$$

Then with κ_j defined from (2.14) and (2.15) as $1/2\ e_{jkm}\,\underline{e}_m\,\underline{e}_k'$, the last term becomes

$$\frac{\partial \kappa_j}{\partial \underline{e}_i'} = \frac{\partial}{\partial \underline{e}_i'}\left[\frac{1}{2}e_{jkm}\underline{e}_m\cdot\underline{e}_k'\right] = \frac{1}{2}e_{jkm}\underline{e}_m\,\delta_{ik} = \frac{1}{2}e_{jim}\underline{e}_m. \tag{2.63}$$

Substituting (2.63) and (2.62) into (2.44) gives

$$\begin{aligned}\mathbf{M} &= \underline{e}_i\times\left[\frac{\partial W}{\partial \kappa_j}\left(\frac{1}{2}e_{jim}\underline{e}_m\right)\right]\\ &= \frac{1}{2}\frac{\partial W}{\partial \kappa_j}e_{jim}\,\underline{e}_i\times\underline{e}_m\\ &= \frac{1}{2}\frac{\partial W}{\partial \kappa_j}e_{jim}\,e_{imk}\,\underline{e}_k\\ &= \frac{1}{2}\frac{\partial W}{\partial \kappa_j}e_{imj}\,e_{imk}\,\underline{e}_k.\end{aligned} \tag{2.64}$$

Using the well known e-δ identity [13],

$$e_{imj}\,e_{imk} = 2\,\delta_{jk}, \tag{2.65}$$

equation (2.64) becomes

$$\mathbf{M} = \frac{\partial W}{\partial \kappa_i}\underline{e}_i. \tag{2.66}$$

As a result, combining (2.66) with (2.61) gives

$$\underline{M} = EI\left(\kappa_2 \underline{e}_2 + \kappa_3 \underline{e}_3\right) + GJ\kappa_1 \underline{e}_1. \tag{2.67}$$

Note also that

$$\kappa_2 \underline{e}_2 + \kappa_3 \underline{e}_3 = \underline{e}_1 \times \left[-\kappa_2 \underline{e}_3 + \kappa_3 \underline{e}_2\right]. \tag{2.68}$$

Recalling (2.6) and (2.15b) gives

$$\underline{e}_i' = \Omega_{kj}(\underline{e}_k \otimes \underline{e}_j)\underline{e}_i = \Omega_{ki}\underline{e}_k = e_{jik}\kappa_j \underline{e}_k. \tag{2.69}$$

Setting i=1, this equation becomes

$$\underline{e}_1' = \kappa_3 \underline{e}_2 - \kappa_2 \underline{e}_3. \tag{2.70}$$

Substituting equations (2.68) and (2.70) into (2.67) and recalling that $\underline{e}_1 = \underline{t}$ gives the final result

$$\underline{M} = EI\,\underline{t} \times \underline{t}' + GJ\kappa_1 \underline{t}, \tag{2.71}$$

where EI and GJ are flexural and torsional rigidity respectively. This is the constitutive relationship which will be used for all subsequent analysis in this thesis. Since κ_2 and κ_3 do not appear explicitly in (2.71) and will not be referred to from this point on, κ_1 will be referred to as simply κ. This particular constitutive relationship supplies an additional first integral which any solution to the rod problem must satisfy. This can be seen as follows.

Taking the first derivative with respect to arc length of (2.71) and combining with equation (2.49) yields

$$\underline{M}' = EI\left[\underline{t} \times \underline{t}'' + \underline{t}' \times \underline{t}'\right] + GJ\kappa' \underline{t} + GJ\kappa \underline{t}', \tag{2.72}$$

where EI and GJ are considered to be constant along the rod. Combining (2.72) with (2.49) gives

$$\underline{F} \times \underline{t} = EI\,\underline{t} \times \underline{t}'' + GJ\kappa'\underline{t} + GJ\kappa\underline{t}'. \tag{2.73}$$

Taking the dot product of both sides of (2.73) with $\underline{t}$ and recalling from (2.51) that $\underline{t}'$ is perpendicular to $\underline{t}$ gives the result that $GJ\kappa' = 0$, or

$$\kappa = \text{const}, \tag{2.74}$$

where κ is the twist per unit length along the rod. Equation (2.74) shows that this twist will remain constant along the entire length of the rod. This will serve as accuracy check which any solution determined by the numerical method developed in the next chapter must satisfy.

2.4 APPLICATION OF EQUILIBRIUM EQUATIONS - HELICAL ROD

In this section the previously derived equilibrium equations will be used to solve the problem of a straight rod twisted into a helix and maintained in this deformed configuration by the application of moments and forces along the initial axis of the rod only. While this problem has already been considered by several authors [1] [2], the analysis is presented to show an application of these equations and to obtain an understanding of the difficulties which arise out of their use. This is the only problem known to the author which combines bending and torsion and has a known analytical solution. As such it will serve as a test case for the numerical solution developed in Chapter 3.

Consider a rod with uniform material properties whose initial tangent vector is

along the global $\underline{E}_3$ axis as shown in Figure 2.1.

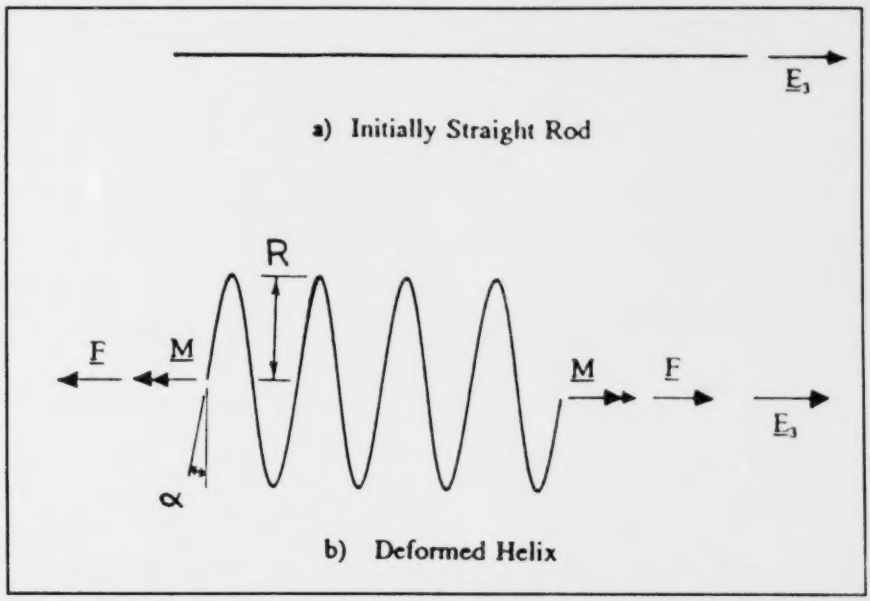

Figure 2.1: Straight Rod Deformed Into a Helix

Here $\{\underline{E}_i\}$ is a fixed global orthonormal basis and $\{\underline{e}_i\}$ is a material orthonormal basis which can change along the length of the rod. At all points, however, $\underline{e}_1 = \underline{t}$ is along the local tangent to the rod. The rod is twisted into a helix of radius R and pitch angle α where α is defined as the angle between the tangent to the spiral and a plane perpendicular to $\underline{E}_3$. The equation of such a helix is

$$\underline{r}(s) = X\underline{E}_1 + Y\underline{E}_2 + Z\underline{E}_3,$$
$$X = R\cos\theta, \quad Y = R\sin\theta, \quad Z = R\theta\tan\alpha, \tag{2.75}$$

which traces its curve along the surface of a cylinder, with radius R, along $\underline{E}_3$. Here X, Y, and Z are measured along the $\underline{E}_1$, $\underline{E}_2$, and $\underline{E}_3$ axes respectively and θ is a measure of the angle of rotation about $\underline{E}_3$. Differentiating (2.75) with respect to arc length gives an

expression for the unit tangent vector as

$$\underline{e}_1 = \underline{t} = -R\frac{d\theta}{ds}\sin\theta\,\underline{E}_1 + R\frac{d\theta}{ds}\cos\theta\,\underline{E}_2 + R\frac{d\theta}{ds}\tan\alpha\,\underline{E}_3. \tag{2.76}$$

Since $\underline{t}$ is a unit vector its magnitude must be unity. Using this fact along with (2.76) gives the result

$$\frac{d\theta}{ds} = \frac{\cos\alpha}{R}, \tag{2.77}$$

which is a constant. Therefore (2.76) becomes

$$\underline{e}_1 = \underline{t} = -\cos\alpha\,\sin\theta\,\underline{E}_1 + \cos\alpha\,\cos\theta\,\underline{E}_2 + \sin\alpha\,\underline{E}_3. \tag{2.78}$$

Taking the derivative of (2.78) and using (2.77) yields

$$\underline{t}' = -\frac{\cos^2\alpha}{R}\cos\theta\,\underline{E}_1 - \frac{\cos^2\alpha}{R}\sin\theta\,\underline{E}_2. \tag{2.79}$$

Substituting (2.79) and (2.76) into (2.71) gives

$$\begin{aligned}\underline{M} = {} & \frac{EI}{R}\left[\cos^3\alpha\,\underline{E}_3 + \sin\alpha\cos^2\alpha\left(\sin\theta\,\underline{E}_1 - \cos\theta\,\underline{E}_2\right)\right] \\ & + GJ\kappa\cos\alpha\left[-\sin\theta\,\underline{E}_1 + \cos\theta\,\underline{E}_2\right] + GJ\kappa\sin\alpha\,\underline{E}_3.\end{aligned} \tag{2.80}$$

Therefore, the moment required to maintain the deformed shape is

$$\underline{M} = M_z\,\underline{E}_3 + M_\theta\,\underline{E}_\theta, \tag{2.81a}$$

where

$$M_z = GJ\kappa\sin\alpha + \frac{EI}{R}\cos^3\alpha, \tag{2.81b}$$

$$M_\theta = GJ\kappa\cos\alpha - \frac{EI}{R}\cos^2\alpha\sin\alpha, \tag{2.81c}$$

and

$$\underline{E}_\theta = -\sin\theta\underline{E}_1 + \cos\theta\underline{E}_2. \tag{2.81d}$$

Note that M_θ is directed along the tangent to the cylinder defined by the helix. From (2.81b) - (2.81d) it can be seen that both M_z and M_θ are constant but the orientation of $\underline{M}_\theta$ changes along the rod. At the start of the rod, $\theta=0$, $\underline{E}_\theta$ is equal to $\underline{E}_2$.

To determine the force required, the derivative of (2.79) is given as

$$\underline{t}'' = \frac{\cos^3\alpha}{R^2}\sin\theta\,\underline{E}_1 - \frac{\cos^3\alpha}{R^2}\cos\theta\,\underline{E}_2. \tag{2.82}$$

Substituting (2.79) and (2.82) into (2.73) and using the result of (2.74) gives

$$\underline{F}\times\underline{t} = \left[\frac{EI}{R^2}\cos^3\alpha\sin\alpha - \frac{GJ\kappa}{R}\cos^2\alpha\right]\left[\cos\theta\underline{E}_1 + \sin\theta\underline{E}_2\right]. \tag{2.83}$$

Therefore, since $\underline{F}\times\underline{t}$ has no component in the $\underline{E}_3$ direction, $\underline{F}$ must be along the Z ($\underline{E}_3$) axis, as expected. Comparing (2.78) and (2.83) gives the force $\underline{F}$ as

$$\underline{F} = F_z\underline{E}_3, \quad F_z = \frac{GJ\kappa}{R}\cos\alpha - \frac{EI}{R^2}\cos^2\alpha\sin\alpha. \tag{2.84}$$

This is the axial force required to maintain the deformed shape. Comparing (2.81c) and (2.84) shows that

$$M_\theta = F_z R. \tag{2.85}$$

Therefore if no axial load is applied the resultant moment is purely along the helix axis.

Some further relations among these variables can be established. Taking the dot product of both sides of (2.71) with $\underline{t}$ gives

$$\underline{M}\cdot\underline{t} = GJ\kappa \tag{2.86}$$

which is satisfied identically when $\underline{M}$ is given by equation (2.81). For the special case where there is no axial force, $\underline{M} = M_z\underline{E}_3$, equation (2.86) gives

$$\kappa = \frac{M_z \sin\alpha}{GJ} \tag{2.87}$$

and equations (2.84) and (2.87) combine to give the radius of the helix as

$$R = \frac{EI}{M_z}\cos\alpha\,. \tag{2.88}$$

CHAPTER

THREE

SEGMENTAL SHOOTING TECHNIQUE

In the previous chapter the equations of equilibrium for an initially straight, inextensible, transversely isotropic rod were developed. These equations were then combined with constitutive assumptions to obtain the equations which describe the rod's deformations. These equations are highly nonlinear and as such are often very difficult to solve analytically. Also, due to the nonlinearity involved, the problems being investigated may also exhibit multiple equilibrium configurations which further complicates the matter [13].

In this chapter a method of solution of these equations, known as the *segmental shooting technique*, is presented. The segmental shooting technique consists of two main components: the segmental approach and the shooting procedure. The segmental approach is based on the fact that equations of equilibrium are greatly simplified when only small deformations occur. These simplified equations and their solution using a power series are shown. To solve rod problems, involving large deformations due to combined bending and torsion, the rod is divided into a finite number of shorter rods called segments. The end of these rod segments undergo only small relative deformations so that the simplified equilibrium equations can be applied over each segment individually. Specifically, knowing the forces and geometry at the beginning of the segment, the solution allows the calculation of the forces and geometry at the end

of the segment. The solution proceeds in this fashion from segment to segment, ensuring that continuity and compatibility are maintained between the segments, until the entire rod is analysed. The segmental approach is an initial value approach which requires that the conditions at the start of the rod be completely specified. Actual problems are generally boundary value problems where some conditions at the start of the rod are unknown while a corresponding number of conditions at the end of the rod are known. The unknowns at the start of the rod must be initially estimated to start the procedure. The shooting procedure is an iterative process to modify the initial estimates of any unknown values at the start of the rod. This is required to ensure that the boundary conditions at the end of the rod can be satisfied.

Previous authors ([7]-[10], [13]) have applied this technique to analyse the bending of rods in two dimensions. The extension of this work to fully three dimensional deformations is presented in this chapter.

3.1 EQUILIBRIUM EQUATIONS FOR SMALL DEFLECTIONS

Recall from Chapter 2 the equilibrium equations governing the rod's deformations are (2.48),

$$\underline{F}' + \underline{b} = \underline{0}, \tag{3.1}$$

(2.49),

$$\underline{M}' = \underline{F} \times \underline{t}, \tag{3.2}$$

as well as the constitutive relationship (2.71),

$$\underline{M} = EI\,\underline{t}\times\underline{t}' + GJ\kappa\underline{t}, \tag{3.3}$$

repeated here for convenience. Consider the arbitrary rod segment shown in Figure 3.1.

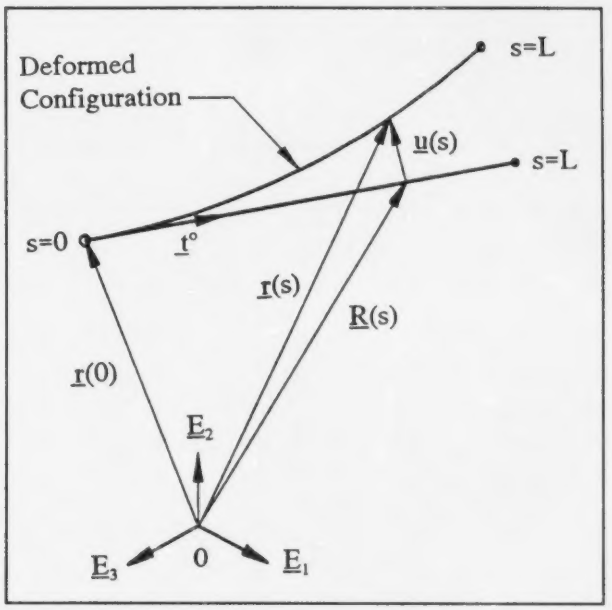

Figure 3.1: Small Deflection of Arbitrary Rod Segment

The deformed shape, $\underline{r}(s)$, can be represented as a deviation $\underline{u}(s)$ from a straight line in the initial tangent direction of the rod segment,

$$\underline{r}(s) = \underline{R}(s) + \underline{u}(s), \tag{3.4}$$

where $\underline{R}(s)$ is the position on the initial straight line corresponding to the same value of arc length, or

$$\underline{R}(s) = \underline{r}(0) + \underline{t}^0 s. \tag{3.5}$$

Here $\underline{r}(0)$ is the location of the start of the rod segment corresponding to zero arc length and $\underline{t}^0$ is in the initial tangent direction of the rod segment. The 0 superscript indicates a vector at the start of the segment corresponding to arc length s=0.

At the start of the segment both the initial straight line and the deformed rod segment are required to have the same position in space, that is $\underline{R}(0)=\underline{r}(0)$. Therefore, from (3.4), there is the initial condition

$$\underline{u}(0) = \underline{0}. \tag{3.6}$$

Taking the derivative of (3.4) with respect to s and using (2.1) and (3.5) gives

$$\underline{r}'(s) = \underline{t}(s) = \underline{t}^0 + \underline{u}'(s), \tag{3.7}$$

where $\underline{R}'(s) = \underline{t}^0$ is the unit vector in the direction of the initial straight line. Since the tangent at the beginning of the segment for both the initial straight line and the deformed shape are required to have the same direction, $\underline{t}^0$, (3.7) furnishes a further initial condition that

$$\underline{u}'(0) = \underline{0}. \tag{3.8}$$

Now let the deviation $\underline{u}(s)$ be represented as

$$\underline{u} = u(s)\,\underline{t}^0 + v(s)\,\underline{e}_2^0 + w(s)\,\underline{e}_3^0, \tag{3.9}$$

where $\{\underline{t}^0;\underline{e}_\alpha{}^0\}$; α=2,3 is an orthonormal basis, constant over the segment, with the $\underline{e}_\alpha{}^0$ spanning the cross section of the rod at the location s=0. Since the rods being considered are inextensible, it follows that $\underline{t}\cdot\underline{t}=1$, or using (3.7),

$$\left(\underline{t}^0 + \underline{u}'(s)\right)\cdot\left(\underline{t}^0 + \underline{u}'(s)\right) = 1 = \underline{t}^0\cdot\underline{t}^0 + 2\underline{t}^0\cdot\underline{u}'(s) + O(|\underline{u}'(s)|^2). \tag{3.10}$$

Then for small deviations $\underline{u}(s)$ this becomes, using (3.9),

$$\underline{t}^0\cdot\underline{u}'(s) = u'(s) = 0. \tag{3.11}$$

Combining this result with the initial condition in (3.6) gives the result u(s)=0 for all values of arc length s. As a result, (3.9) simplifies to

$$\underline{u}(s) = v(s)\,\underline{e}_2^0 + w(s)\,\underline{e}_3^0. \tag{3.12}$$

Equation (3.12) shows that for small deflections, the deviation from the initial undeformed straight shape only has components perpendicular to the original position. The component of the end of the segment in the $\underline{t}^0$ direction is equal to the length of the segment. This assumption is similar to that made in small bending theory of beams.

Taking the first derivative of (3.3) with respect to arc length and combining with (3.2) gives equation (2.73), or

$$\underline{F}\times\underline{t} = EI\,\underline{t}\times\underline{t}'' + GJ\kappa'\underline{t} + GJ\kappa\underline{t}'. \tag{3.13}$$

Then substituting (3.7) into (3.13) gives

$$EI(\underline{t}^0 + \underline{u}')\times\underline{u}''' + GJ\kappa'\left(\underline{t}^0 + \underline{u}'\right) + GJ\kappa\,\underline{u}'' = \underline{F}\times\underline{t}^0 + \underline{F}\times\underline{u}'. \tag{3.14}$$

The force at any point along the rod segment is known from (3.1) if the force at one point and any externally applied loads are known. The force in such a case is given by

$$\underline{F}(s) = \underline{F}(0) - \int_0^s \underline{b}(s)\,ds - \sum_{i=0}^{n} \underline{f}_i, \tag{3.15}$$

where $\underline{b}(s)$ is the total distributed load applied to the rod, $\underline{f}_i$ are the point loads applied on the rod between arc lengths 0 and s and $\underline{F}(s)$ is the resultant contact force applied on the material in [0,s] by the material in (s,L]. Therefore this force can be written as

$$\underline{F}(s) = P(s)\underline{i}^0 + Q(s)\underline{e}_2^0 + R(s)\underline{e}_3^0, \tag{3.16}$$

where P(s), Q(s) and R(s) are known functions of arc length. As well let κ be given as

$$\kappa(s) = \Phi_0 + k(s), \quad k(0) = 0, \tag{3.17}$$

where Φ_0 is the initial twist per unit length of the segment, given by torque/GJ, and k(s) is the variation in twist per unit length which occurs along the length of the segment. Substituting (3.12), (3.16) and (3.17) into (3.14) gives

$$\begin{aligned} EI\left[(v'w''' - w'v''')\underline{i}^0 - w'''\underline{e}_2^0 + v'''\underline{e}_3^0\right] + GJk'\underline{i}^0 + GJ\Phi_0\left[v''\underline{e}_2^0 + w''\underline{e}_3^0\right] - \\ \left[Q(s)w' - R(s)v'\right]\underline{i}^0 + \left[R(s) - P(s)w'\right]\underline{e}_2^0 + \left[P(s)v' - Q(s)\right]\underline{e}_3^0, \end{aligned} \tag{3.18}$$

where v = v(s), w = w(s), k = k(s) and it was assumed that only small deformations occur. This assumption implies that some terms are small relative to some others for the segment (total deflection compared to segment length for example). In order to ensure the retention of the proper terms, a dimensional analysis of this equation was done (Appendix A). Equation (3.18) is the approximate equilibrium equation. Looking at the three components separately gives

$$EI(v'w''' - w'v''') + GJk' = Q(s)w' - R(s)v', \tag{3.19a}$$

$$-EIw''' + GJ\Phi_0 v'' = R(s) - P(s)w', \tag{3.19b}$$

$$EIv''' + GJ\Phi_0 w'' = P(s)v' - Q(s). \tag{3.19c}$$

This is a nonlinear system of equations for v(s) and w(s) due to the mixed terms in (3.19a) due to the coupling between bending and twisting. However, (3.19b) and (3.19c) are two linear differential equations for v(s) and w(s). These equations can be solved using standard methods such as the power series solution presented in the next section. After v(s) and w(s) have been determined, (3.19a) becomes a linear differential equation for k(s), which is the small variation in the twist per unit length along the segment. In essence, the twisting has been uncoupled from the bending for the case of the initially straight rod undergoing small deformations.

It is interesting to note that, according to equation (2.74), the twist per unit length, κ, is constant along the rod, but (3.17) allows a variation in κ to occur. The explanation for this apparent discrepancy is that (2.74) deals with the exact solution while (3.17) is associated with the approximate solution which applies for the case of small deformations. The approximate solution by definition is not identical to the exact solution. Therefore some of the properties of the exact solution cannot be realized by the approximate solution. For example, if κ was assumed to be constant then k(s) (the deviation in κ) would be identically zero. Then equation (3.19a) would be another equation which v and w must satisfy, making a total of three differential equations for two unknown functions which would result in an overdetermined system. With the

approximate approach, small variations in κ must be permitted.

A similar situation occurs in planar bending. A beam which undergoes pure bending will have a constant moment along its length and a constant radius of curvature. However, the linearized bending equation gives the result that d^2w/ds^2 is constant, where w is the transverse deflection of the beam. The condition d^2w/ds^2 = constant implies a parabolic deflected shape while the exact result is a circular arc.

While the exact result, k(s)=0, cannot be applied to the simplified case, the purpose of the procedure is to closely approximate the nonlinear solution, so k(s) is necessarily small. This will be used as an accuracy check on the solutions obtained using the approximate approach.

3.2 POWER SERIES SOLUTION

In this section the equilibrium equations obtained in (3.19a)-(3.19c) are solved using a power series approximation. To do so the equations are first non-dimensionalized so that a general segment may be considered. Consider a segment of the rod of length L shown in Figure 3.2.

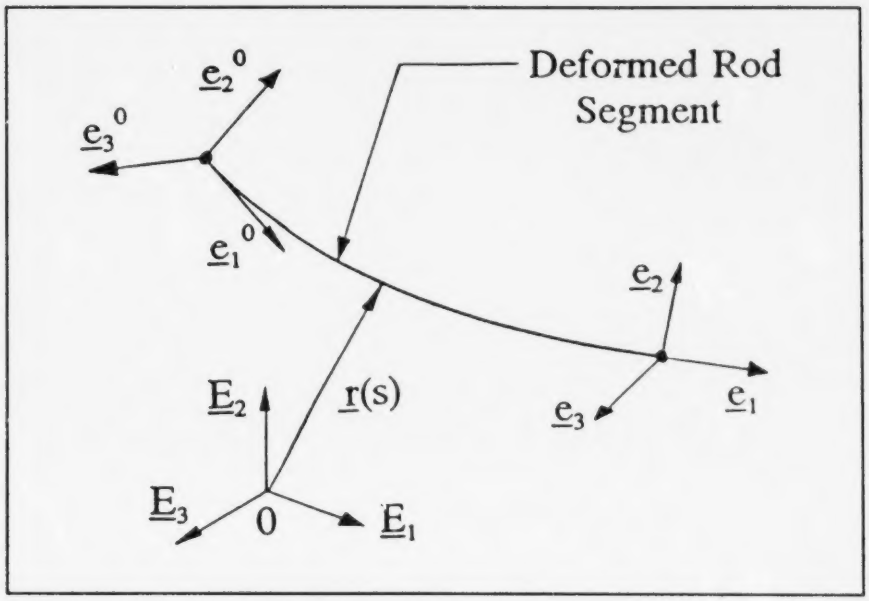

Figure 3.2: Rod Segment

Here $\{\underline{E}_i\}$ is a global orthonormal basis which remains constant, while $\{\underline{e}_i\}$ is an orthonormal basis which consists of embedded material vectors which can change orientation along the length of the rod segment. As described in Chapter Two, $\underline{e}_1$, which is also referred to as $\underline{t}$, is everywhere tangent to the rod curve, while $\underline{e}_2$ and $\underline{e}_3$ span the cross section. At the start of the segment, $\{\underline{e}_i\}$ takes on the values $\{\underline{e}_i^0\}$.

When formulating a particular rod problem the loads, reactions and coordinates will most commonly be expressed in terms of the global basis $\{\underline{E}_i\}$. For example, if the weight of the rod is considered in a problem it will be a dead distributed force in a particular direction, say the negative $\underline{E}_2$ direction. However, as individual segments are being considered in the problem, they will be solved in terms of the basis at the start of that segment, $\{\underline{e}_i^0\}$, referred to as the *local* basis. Thus the weight may have components in all three $\underline{e}_i^0$ directions. It is important therefore that any forces or moments that are

applied to the segment be expressed in terms of $\{\underline{e}_i^0\}$ for that particular segment. Similarly, once the solution for a segment is obtained and the forces and moments are determined at the end of the segment (in terms of $\{\underline{e}_i^0\}$), these as well need to be re-expressed in terms of the new orthonormal basis $\{\underline{e}_i\}$ at the end of the segment which will then be used as the local basis $\{\underline{e}_i^0\}$ for the next segment.

3.2.1 Non-Dimensionalization

Equations (3.19b) and (3.19c) are two third order linear differential equations for v(s) and w(s). These equations can be reduced to second order by defining

$$\delta(s) = \frac{dv(s)}{ds}, \quad \epsilon(s) = \frac{dw(s)}{ds}. \tag{3.20}$$

Note that (3.8) and (3.12) then give the initial conditions

$$\delta(0) = 0, \quad \epsilon(0) = 0. \tag{3.21}$$

Then (3.19c) and (3.19b) become

$$\begin{aligned} EI\frac{d^2\delta}{ds^2} + GJ\Phi_0\frac{d\epsilon}{ds} &= P(s)\delta - Q(s), \\ EI\frac{d^2\epsilon}{ds^2} - GJ\Phi_0\frac{d\delta}{ds} &= P(s)\epsilon - R(s), \end{aligned} \tag{3.22}$$

and similarly (3.19a) becomes

$$GJ\frac{dk}{ds} = Q(s)\epsilon - R(s)\delta + EI\left(\epsilon\frac{d^2\delta}{ds^2} - \delta\frac{d^2\epsilon}{ds^2}\right). \tag{3.23}$$

For the rod segment loaded by uniform distributed loads H_1, H_2 and H_3 in the $\underline{i}^0$, $\underline{e}_2{}^0$ and $\underline{e}_3{}^0$ directions respectively, the forces acting on the cross section of the rod become

$$\begin{aligned} P(s) &= T_0 - H_1 s, \\ Q(s) &= V_{20} - H_2 s, \\ R(s) &= V_{30} - H_3 s, \end{aligned} \tag{3.24}$$

where T_0 is the initial tension in the $\underline{i}^0$ direction and V_{20} and V_{30} are the initial shears in the $\underline{e}_2{}^0$ and $\underline{e}_3{}^0$ directions respectively. Here the 0 subscript indicates values at the start of the rod corresponding to s=0. A uniform distributed load will be useful even for non-uniform loads because in order to solve the problem the rod will be divided into a large number of segments. Over each individual segment the load will then be approximately uniform. Equations (3.22) then become

$$\begin{aligned} EI\delta'' + GJ\Phi_0\epsilon' + V_{20} - H_2 s &= [T_0 - H_1 s]\delta, \\ EI\epsilon'' - GJ\Phi_0\delta' + V_{30} - H_3 s &= [T_0 - H_1 s]\epsilon, \end{aligned} \tag{3.25}$$

and (3.23) becomes

$$GJk' = [V_{20} - H_2 s]\epsilon - [V_{30} - H_3 s]\delta + EI(\epsilon\delta'' - \delta\epsilon''), \tag{3.26}$$

where the $'$ notation again indicates differentiation with respect to arc length.

At this point it is important to remember that these equations are formulated in terms of an orthonormal basis $\{\underline{i}^0, \underline{e}_\alpha{}^0\}$ which is constant over the segment, but will in general be different for different segments. Variables used for this segment, which include tension, shears and distributed loadings, must be expressed in terms of this particular $\{\underline{e}_i{}^0\}$ basis.

In order to non-dimensionalize these equations the following dimensionless parameters are introduced

$$\rho = \frac{s}{L}, \qquad \tau_0 = \frac{T_0 L^2}{EI}, \qquad \nu_{20} = \frac{V_{20} L^2}{EI}, \quad \nu_{30} = \frac{V_{30} L^2}{EI},$$
$$\chi_1 = \frac{H_1 L^3}{EI}, \quad \chi_2 = \frac{H_2 L^3}{EI}, \quad \chi_3 = \frac{H_3 L^3}{EI}, \quad \Delta = \frac{GJ\Phi_0 L}{EI}. \tag{3.27}$$

Multiplying (3.25) and (3.26) by L^2/EI and using the parameters defined in (3.27) gives

$$\frac{d^2\delta}{d\rho^2} + \Delta \frac{d\epsilon}{d\rho} + \nu_{20} - \chi_2 \rho = [\tau_0 - \chi_1 \rho]\delta,$$
$$\frac{d^2\epsilon}{d\rho^2} - \Delta \frac{d\delta}{d\rho} + \nu_{30} - \chi_3 \rho = [\tau_0 - \chi_1 \rho]\epsilon, \tag{3.28}$$

and

$$\frac{\Delta}{\Phi_0}\frac{dk}{d\rho} = [\nu_{20} - \chi_2 \rho]\epsilon - [\nu_{30} - \chi_3 \rho]\delta + \left(\epsilon \frac{d^2\delta}{d\rho^2} - \delta \frac{d^2\epsilon}{d\rho^2}\right). \tag{3.29}$$

To determine the initial values for the variables δ and ϵ, consider the constitutive relationship (2.71),

$$\underline{M} = EI\, \underline{t} \times \underline{t}' + GJ\kappa\, \underline{t}. \tag{3.30}$$

For small deflections, substituting (3.7), (3.12) and (3.17) into (3.30) gives

$$\underline{M} = EI\left[\left(\underline{t}^0 + \frac{dv}{ds}\underline{e}_2^0 + \frac{dw}{ds}\underline{e}_3^0\right) \times \left(\frac{d^2v}{ds^2}\underline{e}_2^0 + \frac{d^2w}{ds^2}\underline{e}_3^0\right)\right]$$
$$+ GJ\,(\Phi_0 + k)\left[\underline{t}^0 + \frac{dv}{ds}\underline{e}_2^0 + \frac{dw}{ds}\underline{e}_3^0\right]. \tag{3.31}$$

At the start of the segment dv/ds, dw/ds and k are zero from equations (3.17) and (3.21) so that (3.31) reduces to

$$\underline{M}(0) = EI\left[-\frac{d^2w}{ds^2}\underline{e}_2^0 + \frac{d^2v}{ds^2}\underline{e}_3^0\right] + GJ\Phi_0\underline{t}^0. \tag{3.32}$$

Thus at the start of the rod the components of the moment in the $\underline{e}_i^0$ directions are given by

$$M_1(0) = GJ\Phi_0, \tag{3.33a}$$

$$M_2(0) = -EI\frac{d^2w}{ds^2}, \tag{3.33b}$$

$$M_3(0) = EI\frac{d^2v}{ds^2}, \tag{3.33c}$$

where the signs are chosen to correspond to (3.32). Equation (3.27) with (3.33b) and (3.33c) furnish the further initial conditions

$$\begin{aligned}\frac{d\epsilon}{d\rho}\Big|_{\rho=0} &= \eta,\\ \frac{d\delta}{d\rho}\Big|_{\rho=0} &= \mu,\end{aligned} \tag{3.34}$$

where η and μ are dimensionless parameters defined as

$$\begin{aligned}\eta &= -\frac{M_2L}{EI}\Big|_{s=0},\\ \mu &= \frac{M_3L}{EI}\Big|_{s=0}.\end{aligned} \tag{3.35}$$

3.2.2 Series Coefficients

To obtain a solution to the equations expressed in (3.28) subject to the initial conditions given in (3.21) and (3.34), δ and ε are assumed to be of the form of a power series

$$\begin{aligned} \delta &= \sum_{k=0}^{\infty} \alpha_k \rho^k, \\ \varepsilon &= \sum_{k=0}^{\infty} \beta_k \rho^k. \end{aligned} \tag{3.36}$$

Substituting (3.36) into (3.28) and using the initial conditions

$$\begin{aligned} \alpha_0 &= 0, \qquad \alpha_1 = \left.\frac{d\delta}{d\rho}\right]_{\rho=0} = \mu, \\ \beta_0 &= 0, \qquad \beta_1 = \left.\frac{d\varepsilon}{d\rho}\right]_{\rho=0} = \eta. \end{aligned} \tag{3.37}$$

gives

$$\begin{aligned} &\sum_{k=2}^{\infty} k(k-1)\alpha_k \rho^{k-2} + \Delta\left(\beta_1 + \sum_{k=2}^{\infty} k\beta_k \rho^{k-1}\right) + \nu_{20} - \chi_2 \rho = (\tau_0 - \chi_1 \rho)\sum_{k=0}^{\infty} \alpha_k \rho^k, \\ &\sum_{k=2}^{\infty} k(k-1)\beta_k \rho^{k-2} - \Delta\left(\alpha_1 + \sum_{k=2}^{\infty} k\alpha_k \rho^{k-1}\right) + \nu_{30} - \chi_3 \rho = (\tau_0 - \chi_1 \rho)\sum_{k=0}^{\infty} \beta_k \rho^k. \end{aligned} \tag{3.38}$$

Collecting the constant (ρ^0) terms yields

$$\begin{aligned} 2\alpha_2 + \Delta\beta_1 + \nu_{20} &= \tau_0 \alpha_0, \\ 2\beta_2 - \Delta\alpha_1 + \nu_{30} &= \tau_0 \beta_0. \end{aligned} \tag{3.39}$$

Similarly for the first order (ρ) terms

$$\begin{aligned} 6\alpha_3 + 2\Delta\beta_2 - \chi_2 &= \tau_0\alpha_1 - \chi_1\alpha_0, \\ 6\beta_3 - 2\Delta\alpha_2 - \chi_3 &= \tau_0\beta_1 - \chi_1\beta_0, \end{aligned} \tag{3.40}$$

and for the ρ^{k-2} terms (k=4,5,6,...)

$$\begin{aligned} k(k-1)\alpha_k + \Delta(k-1)\beta_{k-1} &= \tau_0\alpha_{k-2} - \chi_1\alpha_{k-3}, \\ k(k-1)\beta_k - \Delta(k-1)\alpha_{k-1} &= \tau_0\beta_{k-2} - \chi_1\beta_{k-3}. \end{aligned} \tag{3.41}$$

Therefore, solving (3.39)-(3.41) gives the power series coefficients as

$$\begin{aligned} \alpha_2 &= \tfrac{1}{2}\left[\tau_0\delta(0) - \Delta\eta - \nu_{20}\right], \\ \beta_2 &= \tfrac{1}{2}\left[\tau_0\epsilon(0) + \Delta\mu - \nu_{30}\right], \end{aligned} \tag{3.42}$$

$$\begin{aligned} \alpha_3 &= \tfrac{1}{6}\left[\tau_0\mu - \chi_1\delta(0) - 2\Delta\beta_2 + \chi_2\right], \\ \beta_3 &= \tfrac{1}{6}\left[\tau_0\eta - \chi_1\epsilon(0) + 2\Delta\alpha_2 + \chi_3\right], \end{aligned} \tag{3.43}$$

and

$$\begin{aligned} \alpha_k &= \frac{1}{k(k-1)}\left[\tau_0\alpha_{k-2} - \chi_1\alpha_{k-3} - \Delta(k-1)\beta_{k-1}\right], \\ \beta_k &= \frac{1}{k(k-1)}\left[\tau_0\beta_{k-2} - \chi_1\beta_{k-3} + \Delta(k-1)\alpha_{k-1}\right], \\ k &= 4,5,6\ldots. \end{aligned} \tag{3.44}$$

3.2.3 Deformations, Forces and Moments

The series coefficients can be calculated using equations (3.37) and (3.42)-(3.44). It remains now to calculate the appropriate information required at the end of the

segment which will be used to start the next segment.

The deflections v(s) and w(s) in the $\underline{e}_2^0$ and $\underline{e}_3^0$ directions respectively are given by

$$v(s) = \int_0^s \frac{dv}{ds}\,ds = L\int_0^\rho \delta(\rho)\,d\rho = L\int_0^\rho \left(\sum_{k=0}^{\infty} \alpha_k \rho^k\right) d\rho = L\sum_{k=0}^{\infty} \frac{\alpha_k}{k+1}\,\rho^{k+1},$$
$$w(s) = \int_0^s \frac{dw}{ds}\,ds = L\int_0^\rho \epsilon(\rho)\,d\rho = L\int_0^\rho \left(\sum_{k=0}^{\infty} \beta_k \rho^k\right) d\rho = L\sum_{k=0}^{\infty} \frac{\beta_k}{k+1}\,\rho^{k+1}. \tag{3.45}$$

In (3.45) the integration and summation were interchanged in the last step. This is valid because the integration is actually of a power series represented by a finite polynomial. Each term can be integrated separately and then added together to obtain the total integral. Though the series are shown as infinite polynomials in (3.45), in actual practice the series will be terminated after the coefficients reach a sufficiently small value (a partial sum of 10^{-12} for the last three terms was used). Thus at the end of the segment, $\rho=1$, the deflections are given by

$$v(L) = L\sum_{k=0}^{\infty} \frac{\alpha_k}{k+1},$$
$$w(L) = L\sum_{k=0}^{\infty} \frac{\beta_k}{k+1}. \tag{3.46}$$

Similarly, k(s) is given as

$$k(s) = \int_0^s \frac{dk}{ds}\,ds = L\int_0^\rho \frac{dk}{ds}\,d\rho = L\int_0^\rho \left(\frac{1}{L}\frac{dk}{d\rho}\right) d\rho = \int_0^\rho \frac{dk}{d\rho}\,d\rho. \tag{3.47}$$

Integrating (3.29) once gives

$$k(\rho) = \frac{\Phi_0}{\Delta}\int_0^{\rho}\left(\left[\nu_{20}-\chi_2\rho\right]\epsilon - \left[\nu_{30}-\chi_3\rho\right]\delta\right)d\rho + \frac{\Phi_0}{\Delta}\int_0^{\rho}\left(\epsilon\frac{d^2\delta}{d\rho^2} - \delta\frac{d^2\epsilon}{d\rho^2}\right)d\rho. \tag{3.48}$$

The last integral in (3.48) may be simplified by integrating by parts:

$$\int_0^{\rho}\left(\epsilon\frac{d^2\delta}{d\rho^2}\right)d\rho = \left[\epsilon\frac{d\delta}{d\rho}\right]_0^{\rho} - \int_0^{\rho}\left(\frac{d\epsilon}{d\rho}\frac{d\delta}{d\rho}\right)d\rho,$$
$$\int_0^{\rho}\left(\delta\frac{d^2\epsilon}{d\rho^2}\right)d\rho = \left[\delta\frac{d\epsilon}{d\rho}\right]_0^{\rho} - \int_0^{\rho}\left(\frac{d\delta}{d\rho}\frac{d\epsilon}{d\rho}\right)d\rho. \tag{3.49}$$

Using (3.49) the last integral in (3.48) becomes

$$\int_0^{\rho}\left(\epsilon\frac{d^2\delta}{d\rho^2} - \delta\frac{d^2\epsilon}{d\rho^2}\right)d\rho = \left[\epsilon\frac{d\delta}{d\rho}\right]_0^{\rho} - \left[\delta\frac{d\epsilon}{d\rho}\right]_0^{\rho}, \tag{3.50}$$

Substituting (3.36) into the first integral in (3.48) and recalling k(0)=0 gives

$$k(\rho) = \frac{\Phi_0}{\Delta}\left[\nu_{20}\sum_{k=0}^{\infty}\frac{\beta_k}{k+1}\rho^{k+1} - \chi_2\sum_{k=0}^{\infty}\frac{\beta_k}{k+2}\rho^{k+2} - \nu_{30}\sum_{k=0}^{\infty}\frac{\alpha_k}{k+1}\rho^{k+1} + \chi_3\sum_{k=0}^{\infty}\frac{\alpha_k}{k+2}\rho^{k+2} + \left(\epsilon\frac{d\delta}{d\rho} - \delta\frac{d\epsilon}{d\rho}\right)_0^{\rho}\right]. \tag{3.51}$$

At the end of the segment, $\rho=1$, k is thus

$$k|_{\rho-1} = \frac{EI}{GJL}\left[\nu_{20}\sum_{k=0}^{\infty}\frac{\beta_k}{k+1} - \chi_2\sum_{k=0}^{\infty}\frac{\beta_k}{k+2} - \nu_{30}\sum_{k=0}^{\infty}\frac{\alpha_k}{k+1} + \chi_3\sum_{k=0}^{\infty}\frac{\alpha_k}{k+2} + \left(\epsilon\frac{d\delta}{d\rho} - \delta\frac{d\epsilon}{d\rho}\right)_{\rho-1}\right], \tag{3.52}$$

where using (3.36) the last terms are given by

$$\delta|_{\rho-1} = \sum_{k=0}^{\infty}\alpha_k\left(\rho|_{\rho-1}\right)^k = \sum_{k=0}^{\infty}\alpha_k, \quad \frac{d\delta}{d\rho}|_{\rho-1} = \sum_{k=1}^{\infty}k\alpha_k\left(\rho|_{\rho-1}\right)^{k-1} = \sum_{k=1}^{\infty}k\alpha_k,$$
$$\epsilon|_{\rho-1} = \sum_{k=0}^{\infty}\beta_k\left(\rho|_{\rho-1}\right)^k = \sum_{k=0}^{\infty}\beta_k, \quad \frac{d\epsilon}{d\rho}|_{\rho-1} = \sum_{k=1}^{\infty}k\beta_k\left(\rho|_{\rho-1}\right)^{k-1} = \sum_{k=1}^{\infty}k\beta_k. \tag{3.53}$$

The total twist per unit length at the end of the segment is therefore, from (3.17)

$$\hat{\Phi} = \Phi_0 + k|_{\rho-1}, \tag{3.54}$$

where the last term is given by (3.52). The hat symbol is put on Φ in (3.54) to signify that this term cannot be interpreted as the physical twist per unit length of the rod. The $k(\rho)$ term in (3.54) is a result of the simplification of the equilibrium equations and describes the change in the M_1 component of the moment vector which occurs "in the $\underline{e}_1^0$ direction" which remains constant for the segment and is not, in general, tangent to the rod segment except at the point s=0. This is not the same as the M_1 component of the moment in the $\underline{e}_1(s)$ direction which changes along the segment and is always tangent to the rod segment. To determine the physical twist per unit length at the end of the segment it is necessary to express the moments obtained at the end of the segment in terms of the basis obtained at the end of the segment. Then Φ is obtained from M_1/GJ as before. This is discussed in greater detail in Section 3.3.

Having determined the local coordinates, v(s) and w(s), of the end of the segment,

the global coordinates are obtained by combining equations (3.4), (3.5) and (3.12) to get

$$\mathbf{r}(s) = \mathbf{r}(0) + \underline{e}_1^0 s + v(s)\,\underline{e}_2^0 + w(s)\,\underline{e}_3^0, \tag{3.55}$$

as shown in Figure 3.3.

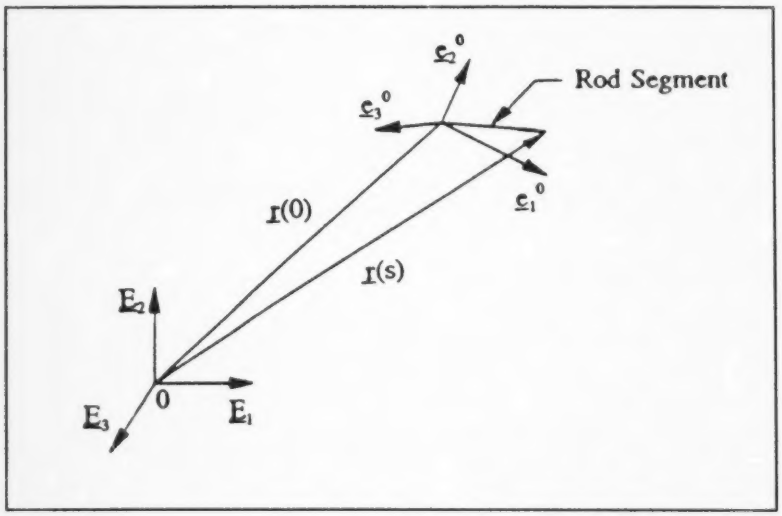

Figure 3.3: Coordinates at End of Segment

The components of $\{\underline{e}_i^0\}$ can be expressed in terms of the global basis $\{\underline{E}_i\}$ as

$$\underline{e}_i^0 = \left(\underline{e}_i^0 \cdot \underline{E}_j\right)\underline{E}_j, \tag{3.56}$$

where the repeated j subscript indicates summation on j from 1 to 3. Then, with $\underline{e}_i^0(j)$ defined as $\underline{e}_i^0 \cdot \underline{E}_j$, combining (3.55) with (3.56) gives the coordinates at the end of the segment (s=L) as

$$X = X_0 + \left[L\, e_1^0(1) + v(L)\, e_2^0(1) + w(L)\, e_3^0(1) \right],$$

$$Y = Y_0 + \left[L\, e_1^0(2) + v(L)\, e_2^0(2) + w(L)\, e_3^0(2) \right], \tag{3.57}$$

$$Z = Z_0 + \left[L\, e_1^0(3) + v(L)\, e_2^0(3) + w(L)\, e_3^0(3) \right],$$

where the components of $\underline{r}(0)$ are $\{X_0, Y_0, Z_0\}$ in the $\underline{E}_1$, $\underline{E}_2$, and $\underline{E}_3$ directions respectively and v(L) and w(L) are obtained from (3.46).

The next step is to determine the new orthonormal basis at the end of the segment. This is necessary because this new basis will be used as the local basis for the next segment. To determine this new basis, first the tangent direction is needed. Recall from (3.7) that

$$\underline{t}(s) = \underline{t}^0 + \underline{u}'(s). \tag{3.58}$$

Then combining (3.12) and (3.58) gives

$$\underline{t}(s) = \underline{t}^0 + \frac{dv}{ds}\underline{e}_2^0 + \frac{dw}{ds}\underline{e}_3^0. \tag{3.59}$$

Using the definition in (3.20) this gives the result that at the end of the segment

$$\underline{t} = \underline{t}^0 + (\delta|_{\rho-1})\underline{e}_2^0 + (\epsilon|_{\rho-1})\underline{e}_3^0, \tag{3.60}$$

where $\delta|_{\rho-1}$ and $\varepsilon|_{\rho-1}$ are given by equation (3.53). The tangent vector given in (3.60) is no longer exactly a unit vector, but is somewhat larger than unity. In order to maintain orthonormality $\underline{t}$, as given in (3.60), is normalized to maintain a unit length.

Having determined the tangent vector $\underline{t}$, $\underline{e}_2$ and $\underline{e}_3$ are then selected to obtain an orthonormal basis. The exact orientations of $\underline{e}_2$ and $\underline{e}_3$ are not important. The only requirement is that they span the cross section of the rod and are perpendicular to each

other. The are an infinite number of vectors $\underline{e}_2$ and $\underline{e}_3$ which satisfy this requirement. One possible choice is to use the Frenet basis, consisting of a tangent vector $\underline{t}$, a normal vector $\underline{n}$ which lies in the principal plane defined by $\underline{t}$ and $\underline{t}'$, and a binormal vector given by $\underline{t}\times\underline{n}$. The Frenet basis is uniquely defined only when the segment does not remain straight. For the special case where the segment remains straight, the same orthonormal basis $\{\underline{e}_i^0\}$ which was used at the beginning of the segment can be used again for the next segment.

For the case where the rod segment does not remain straight (Frenet basis is uniquely defined), the binormal can be approximated by the cross product of $\underline{t}^0$ and $\underline{t}$,

$$\underline{e}_3 = \underline{t}^0 \times \underline{t}, \tag{3.61}$$

and normalizing to obtain a unit length. Here the principal plane is assumed to contain the vectors $\underline{t}^0$ and $\underline{t}$ (and therefore $\underline{t}'$ in the limit as $s\rightarrow 0$) and the binormal vector is perpendicular to this plane. Then the normal vector $\underline{e}_2$ is obtained from

$$\underline{e}_2 = \underline{e}_3 \times \underline{t} \tag{3.62}$$

so that $\{\underline{t};\underline{e}_\alpha\}$ forms a new orthonormal basis at the end of the segment. Other choices of $\underline{e}_2$ and $\underline{e}_3$ are also possible. These are discussed in Appendix B.

Having determined the new basis, the next step is to determine the forces and moments acting on the end of the segment. The forces can be determined from (3.24) where P(s), Q(s) and R(s) are in the $\underline{e}_1^0$, $\underline{e}_2^0$ and $\underline{e}_3^0$ directions respectively. Let $\underline{F}(s)$ be defined as the force vector {P, Q, R}. Then using (3.24) the components of the force vector at the end of the segment (s=L) are given by

$$
\begin{aligned}
F(1) &= T - T_0 - H_1 L, \\
F(2) &= V_2 - V_{20} - H_2 L, \\
F(3) &= V_3 - V_{30} - H_3 L,
\end{aligned}
\tag{3.63}
$$

where F(i) is the component of the force vector in the $\underline{e}_i^\circ$ direction. These components will also be referred to as T, V_2 and V_3 (the tension along the axis of the rod and the two shear forces in the $\underline{e}_2^\circ$ and $\underline{e}_3^\circ$ directions respectively). Multiplying equation (3.63) by L^2/EI gives

$$
\begin{aligned}
\frac{TL^2}{EI} &= \frac{T_0 L^2}{EI} - \frac{H_1 L^3}{EI}\rho, \\
\frac{V_2 L^2}{EI} &= \frac{V_{20} L^2}{EI} - \frac{H_2 L^3}{EI}\rho, \\
\frac{V_3 L^2}{EI} &= \frac{V_{30} L^2}{EI} - \frac{H_3 L^3}{EI}\rho.
\end{aligned}
\tag{3.64}
$$

Then non-dimensionalizing according to (3.27) yields

$$
\begin{aligned}
\tau &= \tau_0 - \chi_1 \rho, \\
v_2 &= v_{20} - \chi_2 \rho, \\
v_3 &= v_{30} - \chi_3 \rho.
\end{aligned}
\tag{3.65}
$$

Thus at the end of the segment (ρ=1) the non-dimensionalized forces are

$$
\begin{aligned}
\tau &= \tau_0 - \chi_1, \\
v_2 &= v_{20} - \chi_2, \\
v_3 &= v_{30} - \chi_3,
\end{aligned}
\tag{3.66}
$$

where χ_1, χ_2 and χ_3 are the dimensionless uniform distributed loads in the $\underline{e}_1^0$, $\underline{e}_2^0$ and $\underline{e}_3^0$ directions respectively.

To determine the moments at the end of the segment, recall that equation (3.31) is the expression for the moments for the case of small deflections. At the end of the segment, this becomes

$$\begin{aligned} \underline{M} = EI\left[\left(\underline{t}^0 + \delta\,\underline{e}_2^0 + \epsilon\,\underline{e}_3^0\right)\times\left(\frac{d\delta}{ds}\underline{e}_2^0 + \frac{d\epsilon}{ds}\underline{e}_3^0\right)\right] \\ + GJ(\Phi_0 + k)\left[\underline{t}^0 + \delta\,\underline{e}_2^0 + \epsilon\,\underline{e}_3^0\right]. \end{aligned} \tag{3.67}$$

With δ and ϵ given in (3.36) the derivatives $(d\delta/ds)$ and $(d\epsilon/ds)$ become

$$\begin{aligned} \frac{d\delta}{ds} &= \frac{1}{L}\frac{d\delta}{d\rho} = \frac{1}{L}\sum_{k=1}^{\infty} k\alpha_k\rho^{k-1}, \\ \frac{d\epsilon}{ds} &= \frac{1}{L}\frac{d\epsilon}{d\rho} = \frac{1}{L}\sum_{k=1}^{\infty} k\beta_k\rho^{k-1}, \end{aligned} \tag{3.68}$$

and at the end of the segment these become

$$\begin{aligned} \left.\frac{d\delta}{ds}\right]_{\rho=1} &= \frac{1}{L}\sum_{k=1}^{\infty} k\alpha_k, \\ \left.\frac{d\epsilon}{ds}\right]_{\rho=1} &= \frac{1}{L}\sum_{k=1}^{\infty} k\beta_k. \end{aligned} \tag{3.69}$$

Substituting (3.52), (3.53) and (3.69) into (3.67) and ignoring the higher order terms gives the components of the moment at the end of the segment as

$$M_1 = GJ(\Phi_0 + k) + EI\left(\delta \frac{d\epsilon}{ds} - \epsilon \frac{d\delta}{ds}\right),$$

$$M_2 = -EI\frac{d\epsilon}{ds} + GJ\Phi_0\delta, \qquad (3.70)$$

$$M_3 = EI\frac{d\delta}{ds} + GJ\Phi_0\epsilon,$$

where once again the components of the moment are expressed in terms of the initial orthonormal basis $\{\underline{e}_i^0\}$. Again, to ensure the retention of proper terms, a dimensional analysis of this equation was performed (Appendix A).

3.3 SOLUTION PROCEDURE

So far in this chapter, the nonlinear equations governing the rod segment's deformation, obtained in Chapter 2, were simplified by assuming that only small deformations occur about an initial straight line. The resulting differential equations were then solved by the use of power series. In this section the use of these segments to solve three dimensional rod problems involving large deflections and rotations due to bending and torsion is discussed. This approach has been applied previously by several authors to analyse planar bending of rods which does not involve torsion [7]-[10], [13]. This section extends this approach, referred to as the *segmental technique*, to fully three dimensional problems.

To demonstrate how the procedure works, consider a rod which is acted upon by forces and moments sufficient to cause the ends of the rod to undergo large deformations. Such a deformation is governed by the fully nonlinear equilibrium equations developed in Chapter 2. To solve such a problem using the segmental

technique, the rod is initially divided into a large number of segments. In doing so, each small segment of the rod will experience only small deformations relative to its neighboring segments. If a sufficient number of such segments are employed then the relative deformations between neighboring segments will be small enough so that the solution for small deflections obtained in the previous sections can be applied over each individual segment.

The solution obtained with the equations developed previously has the effect of converting the original boundary value problem into a sequence of initial value problems. In obtaining the small deflection solution, it was assumed that all variables (forces, moments and geometry) were known at the beginning of the segment. With these initial values given, the corresponding values at the end of the segment can be determined. In particular, if the forces, moments and geometry at the start of a segment are specified then the corresponding forces, moments and geometry at the end of the segment can be obtained. These values at the end of the segment will then be used to start the next segment. The solution of the rod proceeds in this fashion from segment to segment, ensuring that geometric continuity and force compatibility between the segments is maintained, until the entire rod has been analysed.

To use the segmental technique the conditions at the start of the first segment must be completely specified. Actual problems, however, are usually of a boundary value type where some of the variables at the start of the rod are unknown and a corresponding number of variables at the end of the rod are known (eg. zero moment at a free end). To solve such problems with the segmental approach, a *shooting procedure* has been employed by previous authors [7]-[10], [13] for planar problems where the

unknown quantities at the start of the rod are initially assumed. The rod is then solved, segment by segment, and the values obtained at the end of the rod are compared to the known boundary conditions. The initial guesses are then modified iteratively using a Newton-Raphson false position algorithm. This procedure is repeated until the values obtained at the end of the rod converge, within specified tolerances, to the desired boundary conditions to give the appropriate solution. The shooting procedure is discussed in greater detail in Section 3.4.

To start the solution initially, a suitable global orthonormal basis $\{\underline{E}_i\}$ is chosen. Here $\{\underline{E}_i\}$ is a constant orthonormal basis, referred to as the global basis, which is independent of arc length. Also, the rod properties (flexural rigidity, torsional rigidity, length) are known as well as any concentrated or distributed loads acting on the rod. Furthermore, the geometry, forces and moments at the start of the rod are specified. It should be noted that depending on the particular problem being solved, some of these values will be known and some will be initial estimates of unknown values. All forces, moments and distributed loads will usually be most conveniently expressed in terms of the global basis $\{\underline{E}_i\}$.

With the forces acting on the rod known and the initial conditions specified, the rod is then divided into a large number of segments. The number of segments required will depend on the specific problem being considered, but will in general increase with an increase in the total deformation of the rod since the purpose of dividing the rod into segments is to ensure that each segment undergoes only a small relative deformation. To start the solution of the first segment, the initial requirement is to determine a suitable orthonormal basis $\{\underline{e}_i^0\}$ at the start of the segment with $\underline{e}_1^0$ along the tangent of the rod

and with $\underline{e}_2^0$ and $\underline{e}_3^0$ spanning the cross section as discussed in Section 3.2.3. In order to do this, the tangent direction $\underline{t}^0$ is first selected. This will either be specified by the problem or will be an initial unknown which must be estimated. Then $\underline{e}_2^0$ and $\underline{e}_3^0$, which are selected such that $\underline{t}^0$, $\underline{e}_2^0$ and $\underline{e}_3^0$ form a right handed orthonormal basis. There will be an infinite number of choices for $\underline{e}_2^0$ and $\underline{e}_3^0$ which satisfy this requirement and one pair is chosen arbitrarily. This basis will be referred to as the local basis and will be constant for the segment being considered. Then the initial forces and moments, which are most likely to be expressed in terms of the global basis $\{\underline{E}_i\}$, need to be re-expressed in terms of this local basis $\{\underline{e}_i^0\}$. This is necessary because the linearized equations are formulated in terms of the $\{\underline{e}_i^0\}$ basis and any variables associated with this segment must be expressed in terms of this basis. As an example of this transformation, suppose the force vector is given as

$$\underline{F} = F_1^G \underline{E}_1 + F_2^G \underline{E}_2 + F_3^G \underline{E}_3, \tag{3.71}$$

where the G superscript indicates components corresponding to the global $\{\underline{E}_i\}$ basis. Since $\{\underline{e}_i^0\}$ is also a valid basis, the force can also be expressed as

$$\underline{F} = F_1^L \underline{e}_1^0 + F_2^L \underline{e}_2^0 + F_3^L \underline{e}_3^0, \tag{3.72}$$

where the L superscript indicates components corresponding to the local $\{\underline{e}_i^0\}$ basis. The vectors $\underline{E}_i$ can be individually expressed in terms of $\{\underline{e}_i^0\}$ as

$$\underline{E}_i = \left(\underline{E}_i \cdot \underline{e}_j^0\right) \underline{e}_j^0. \tag{3.73}$$

Substituting (3.73) into (3.71) and comparing with (3.72) gives the result

$$F_1^L = F_1^G \underline{E}_1(1) + F_2^G \underline{E}_2(1) + F_3^G \underline{E}_3(1),$$

$$F_2^L = F_1^G \underline{E}_1(2) + F_2^G \underline{E}_2(2) + F_3^G \underline{E}_3(2), \qquad (3.74)$$

$$F_3^L = F_1^G \underline{E}_1(3) + F_2^G \underline{E}_2(3) + F_3^G \underline{E}_3(3),$$

where $\underline{E}_i(j)$ has been defined previously as $\underline{E}_i \cdot \underline{e}_j^0$. This type of transformation will also be applied to the moments and distributed loadings so that all variables pertaining to the first segment are now expressed in terms of the basis $\{\underline{e}_i^0\}$.

Having done this, the first segment is then solved by the method outlined in Sections 3.1 and 3.2. with the forces, moments and geometry at the end of the segment being computed. As well, a new orthonormal basis, $\{\underline{e}_i\}$, with $\underline{e}_1$ along the tangent to the segment is determined at the end of the segment. These values will then be used to start the solution for the next segment. The coordinates determined at the end of the previous segment are expressed in terms of the global $\{\underline{E}_i\}$ basis. The next segment will begin at this location so that geometric continuity is maintained. The forces and moments, however, determined at the end of the previous segment are expressed in terms of the local $\{\underline{e}_i^0\}$ basis. To analyze the next segment, which will use $\{\underline{e}_i\}$ as its local basis to maintain continuity of the slope, the forces and moments need to be re-expressed in terms of this new basis. This is accomplished with a transformation similar to the example shown in equations (3.71)-(3.74) with $\{\underline{e}_i\}$ replacing $\{\underline{e}_i^0\}$ and $\{\underline{e}_i^0\}$ replacing $\{\underline{E}_i\}$. As before, any distributed loadings (which will usually be expressed in terms of the global $\{\underline{E}_i\}$ basis) again need to be expressed in terms the $\{\underline{e}_i\}$ basis which will be used as the $\{\underline{e}_i^0\}$ basis for the next segment. When all this has been completed, the next segment is ready to be solved in a manner similar to the first segment. The forces and

moments determined at the end of the previous segment, in terms of $\{\underline{e}_i\}$, are used as the initial values for the next segment. This follows because these forces and moments are those acting on the material in [0,s] due to the material in (s,L] according to the sign convention employed. Since force continuity is to be maintained between the segments, the forces acting on the end of the previous segment must be the same as those acting at the start of the next segment which is physically in the same location.

The solution proceeds in this manner until all the segments which comprise the total rod have been analysed and the forces, moments and geometry at the end of the rod have been determined. At this point these values are compared to known boundary values and, if necessary, the estimates of the initial unknown values are modified accordingly. This portion of the solution, called the shooting procedure, is discussed in greater detail in the next section.

In previous sections, forces, moments and distributed loads expressed in terms of one basis have been re-expressed in terms of another basis. It should be noted here that such transformations can be carried out with the non-dimensionalized forms of the variables involved. This is more convenient between segments which are solved in terms of dimensionless quantities. For example, the transformation of the force vector shown in (3.71)-(3.74) could have been carried out with the non-dimensionalized values of the components as defined by (3.27). This presents no added difficulties, but it should be noted that when the moments are transformed in this manner, the dimensionless component in the $\underline{e}_2$ direction, η, is defined as $-M_2L/EI$ in equation (3.35). Therefore when transforming the dimensionless moments between bases, the signs of η components must be negative in accordance with the non-dimensionalization expressed in (3.35).

3.4 SHOOTING PROCEDURE

As was mentioned previously, the segmental technique requires that all variables at the start of the first segment be specified in order to obtain a solution. In many problems some of the initial values will be unknown while a corresponding number of values at the end of the rod will be known. The unknowns at the start of the rod must be initially estimated. The shooting procedure is an iterative method used to modify these estimates of the initial unknowns so that the boundary conditions at the end of the rod are satisfied. In what follows it will be assumed that there are N unknown values at the start of the rod while N values at the end of the rod are known boundary values.

Let $\underline{A}$ be an N×1 vector containing the initial estimates of the unknowns at the start of the rod, $\underline{B}$ be an N×1 vector containing the N known boundary values and $\underline{C}$ be an N×1 vector containing the values delivered by the segmental solution corresponding to the known boundary values. The difference between the known boundary values and the values obtained with the segmental solution is the vector difference between $\underline{B}$ and $\underline{C}$, or

$$\underline{E}^k = \underline{B} - \underline{C}^k. \tag{3.75}$$

$\underline{E}^k$ is called the error vector where the superscript k is an iteration counter. The components of $\underline{C}^k$ (the computed values) depend on the initial guesses which are the components of $\underline{A}^k$. Therefore the error vector can be expressed as a function of the components of $\underline{A}^k$, or

$$E^k = E(A^k) = E(A_1^k, A_2^k, ..., A_N^k). \tag{3.76}$$

To obtain a solution to the initial rod problem which satisfies the required boundary conditions it is necessary that each component of the error vector $\underline{E}$ approach zero. Thus the problem of determining the correct initial guesses involves solving a set of N nonlinear equations to determine the components of $\underline{A}$ for which the error vector $\underline{E}$ is approximately zero. A Newton Raphson iterative procedure is used to accomplish this objective. The Newton Raphson method is based on a first order Taylor series which can be written in matrix form as

$$\underline{E}^{k+1} = \underline{E}^{k} + [J]^{k} (\underline{A}^{k+1} - \underline{A}^{k}), \tag{3.77}$$

where $\underline{A}^{k+1}$ are the new values of the initial estimates for the $k+1^{th}$ iteration and $\underline{E}^{k+1}$ are the corresponding values of the components of the error vector. $[J]^{k}$ is the N×N Jacobian matrix, the components of which are given by

$$J_{mn}^{k} = \frac{\partial E_{m}^{k}}{\partial A_{n}^{k}}, \qquad m,n = 1,2,...,N. \tag{3.78}$$

For the rod problems being considered here, the functions E_{m}^{k} are not analytical so the partial derivatives need to be evaluated numerically. A false position backward difference formulation is used to evaluate these derivatives. The approximate partial derivatives are

$$J_{mn}^{k} = \frac{\partial E_{m}^{k}}{\partial A_{n}^{k}} \approx \frac{E_{m}(\underline{A}^{k}) - E_{m}(A_{1}^{k}, A_{2}^{k}, ..., A_{n}^{k} - h, ..., A_{N}^{k})}{h}, \tag{3.79}$$

where h is a small change in A_{n}.

Setting $\underline{E}^{k+1}$ to zero in (3.77) and solving for the new improved initial estimates of the unknown values at the start of the rod gives

$$[J]^k \underline{D} = -\underline{E}^k, \qquad \underline{D} = \underline{A}^{k+1} - \underline{A}^k, \tag{3.80}$$

which can be solved for $\underline{D}$ using standard methods such as Gauss elimination. Having obtained $\underline{D}$, the new initial guesses are then obtained from

$$\underline{A}^{k+1} = \underline{A}^k + \underline{D}. \tag{3.81}$$

The new values of $\underline{A}$ are then used to start the solution over again for the $k+1^{th}$ iteration. This procedure is continued until the error vector approaches zero to within some specified tolerance.

CHAPTER

FOUR

VERIFICATION AND RESULTS

In the previous chapter, the nonlinear equations of equilibrium obtained in Chapter 2 were simplified for the case where only small deformations occur. A solution of these equations was then obtained for a short segment of the rod which met the requirement of small deformations. A method for assembling numerous segments together, maintaining continuity and compatibility, to form a solution for the entire rod was presented, as well as a shooting procedure to ensure that the appropriate boundary conditions are satisfied. This method, known as the *segmental shooting technique*, has been found to be effective by previous authors for planar elastica problems [7]-[10], [13].

In this chapter the segmental shooting technique is used to solve a rod problem which has a known analytical solution to verify the accuracy of the technique. The problem considered is an initially straight rod with a circular cross section twisted into a helical spiral. The analytical solution to this problem is well known and is presented in Section 2.4. This is the only truly three dimensional problem known to this author which has an analytical solution. As well, a demonstration of the shooting procedure is shown for the same problem which is posed with a single unknown at the start of the rod.

4.1 HELICAL ROD

In Section 2.4 the nonlinear equations of equilibrium were applied to the problem of an initially straight rod with circular cross section twisted into a helical spiral under the action of end moments and axially applied forces. This problem has been considered by several authors ([1],[2]) and is the only problem known to this author that combines torsion and bending in a fully three dimensional problem which has a known analytical solution. As such, it will serve as a test case to verify the results obtained using the segmental shooting technique. In addition this example shows some of the details involved in applying this technique to a practical problem.

The problem considered, shown in Figure 2.1, is repeated here for convenience.

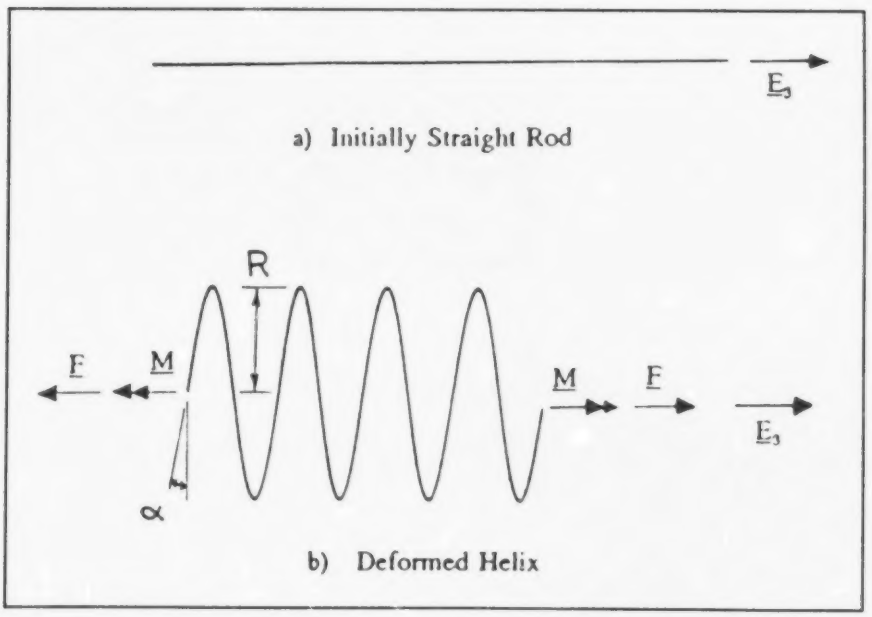

Figure 4.1: Straight Rod Deformed Into A Helix

In this problem the force $\underline{F}$ and moment $\underline{M}$ will be those defined in equations (2.84) and (2.81) respectively and will be assumed to be specified. To obtain a solution to the problem it is also necessary to specify a pitch angle α. With the moment and pitch angle thus specified, κ, the twist per unit length along the rod, and the radius R can be determined from equation (2.81) in general or from (2.87) and (2.88) respectively for the case where $\underline{F} = \underline{0}$. The entire analytical solution is then given in Section 2.4.

To obtain a solution using the segmental technique the conditions at the start of the rod (arc length $s = 0$) must be specified. The starting location (coordinates) of the rod in the global $\{\underline{E}_i\}$ basis must also be specified. The global basis $\{\underline{E}_i\}$ will be defined by the unit vectors

$$\begin{aligned} \underline{E}_1 &= (1, 0, 0), \\ \underline{E}_2 &= (0, 1, 0), \\ \underline{E}_3 &= (0, 0, 1). \end{aligned} \tag{4.1}$$

In this basis the equation of the helix is given by (equation (2.75)),

$$\begin{gathered} \underline{r}(s) = X\underline{E}_1 + Y\underline{E}_2 + Z\underline{E}_3, \\ X = R\cos\theta, \quad Y = R\sin\theta, \quad Z = R\theta\tan\alpha. \end{gathered} \tag{4.2}$$

In addition equation (2.77) can be rearranged to give

$$d\theta = \frac{\cos\alpha}{R}\, ds, \tag{4.3}$$

and when integrated,

$$\theta = \frac{\cos\alpha}{R}\, s + \text{constant}, \tag{4.4}$$

which relates the arc length parameter s to the angle of rotation θ about $\underline{E}_3$ (the Z axis). At the start of the rod assume that $\theta=0$ so (4.4) becomes

$$\theta = \frac{\cos\alpha}{R} s. \tag{4.5}$$

Thus the coordinates of the start of the rod ($s=0$, $\theta=0$) are given by (4.2) as

$$X = R, \quad Y = 0, \quad Z = 0. \tag{4.6}$$

where R is determined from equation (2.81) in general or from (2.88) for the special case of no axial force.

To begin the segmental technique it is necessary to determine a suitable local orthonormal basis $\{\underline{e}_i^0\}$ which will be used as the basis to solve the first segment. Recall from (2.78) that the tangent to the rod is given by

$$\underline{e}_1 = \underline{t} = -\cos\alpha \sin\theta \underline{E}_1 + \cos\alpha \cos\theta \underline{E}_2 + \sin\alpha \underline{E}_3. \tag{4.7}$$

Thus at the start of the rod ($s=0$, $\theta=0$) the $\underline{e}_1^0$ vector is given by

$$\underline{e}_1^0 = \cos\alpha \underline{E}_2 + \sin\alpha \underline{E}_3. \tag{4.8}$$

The vectors $\underline{e}_2^0$ and $\underline{e}_3^0$ are not unique, but must satisfy the condition that $\{\underline{e}_i^0\}$ be a right-handed orthonormal basis. A convenient choice for these vectors at the start of the rod is then

$$\begin{aligned} \underline{e}_2^0 &= \underline{E}_1, \\ \underline{e}_3^0 &= \sin\alpha \underline{E}_2 - \cos\alpha \underline{E}_3. \end{aligned} \tag{4.9}$$

Once the local basis at the start of the first segment has been determined the force and moment vectors need to be expressed in terms of this basis. For the force, $\underline{F} = F\underline{E}_3$, the components of this vector in terms of $\{\underline{e}_i^0\}$ are given by

$$\begin{aligned} F_1^L &= \underline{F}\cdot\underline{e}_1^0 = (F_z\underline{E}_3)\cdot(\cos\alpha\,\underline{E}_2 + \sin\alpha\,\underline{E}_3) = F_z\sin\alpha, \\ F_2^L &= \underline{F}\cdot\underline{e}_2^0 = (F_z\underline{E}_3)\cdot(\underline{E}_1) = 0, \\ F_3^L &= \underline{F}\cdot\underline{e}_3^0 = (F_z\underline{E}_3)\cdot(\sin\alpha\,\underline{E}_2 - \cos\alpha\,\underline{E}_3) = -F_z\cos\alpha. \end{aligned} \tag{4.10}$$

where the L superscript indicates components with respect to the local basis $\{\underline{e}_i^0\}$. Similarly the components of the moment $\underline{M}$ at the start of the rod (θ=0) are given by

$$\begin{aligned} M_1^L &= M_z\sin\alpha + M_\theta\cos\alpha, \\ M_2^L &= 0, \\ M_3^L &= -M_z\cos\alpha + M_\theta\sin\alpha. \end{aligned} \tag{4.11}$$

As well, if there were any distributed loadings acting on the rod (eg. gravity) these would again need to be expressed in terms of the local basis $\{\underline{e}_i^0\}$ in a similar fashion. Since in this case there are no distributed loadings, the relevant components are given by

$$H_1^L = 0, \quad H_2^L = 0, \quad H_3^L = 0. \tag{4.12}$$

The conditions at the start of the rod are therefore specified by equations (4.6) and (4.8)-(4.12) along with R determined from equation (2.81) or (2.84). Given these initial values, which are exact, the segmental approach can then be used to generate the deformed shape of the rod as well as determine the forces and moments at any point along the rod. These can then be compared to the known analytical solution to determine the accuracy of the method. Note that since all initial values are exactly

specified, the iterative shooting procedure is not required here.

4.1.1 Helix With No Axial Forces

Consider an initially straight steel rod with the following properties:

Length = 1 m,	Diameter = 6 mm,
E = 207 GPa,	G = 70 GPa,
EI = 13.16877 Nm^2,	GJ = 8.90642 Nm^2.

Initially consider the case where only moments are applied (ie: axial force $\underline{F}$ is zero). Then from (2.81) and (2.85) the moment is purely axial, $\underline{M} = M_z \underline{E}_3$. For this case M_z and the pitch angle α are arbitrarily selected to be 200 Nm and 45 degrees respectively. Since there is no axial force, the radius of the deformed helix can be obtained from equation (2.88) to be 0.0465586 m. Table 4.1 shows the calculated geometry at the end of the rod obtained with the segmental technique for an increasing number of segments. The analytical solution obtained from (4.2) is also shown. It can be seen for this particular problem that when approximately 500 segments are used the two solutions show excellent agreement. This is further demonstrated in Figures (4.2a)-(4.2c) which show both the analytical solution and the segmental solution obtained using 500 segments. As can be seen from these figures, there is no noticeable difference between the solutions. Table 4.1 also shows that the agreement between the two solutions improves as the number of segments is increased.

Table 4.1: Geometry at the End of a Deformed Helix, M_z=200 Nm, α=45°

# of Segments	X/L	Y/L	Z/L	$\underline{e}_1(3)$
10	-0.000889	-0.066531	0.280631	0.410669
20	0.051239	0.106357	0.637182	0.412292
50	-0.037311	0.038021	0.711142	0.703440
100	-0.039889	0.026341	0.709272	0.708583
200	-0.040289	0.023883	0.707794	0.707768
500	-0.040378	0.023265	0.707231	0.707241
1000	-0.040389	0.023182	0.707139	0.707143
2000	-0.040392	0.023162	0.707115	0.707116
5000	-0.040392	0.023156	0.707108	0.707108
Analytical Result	-0.040393	0.023155	0.707107	0.707107

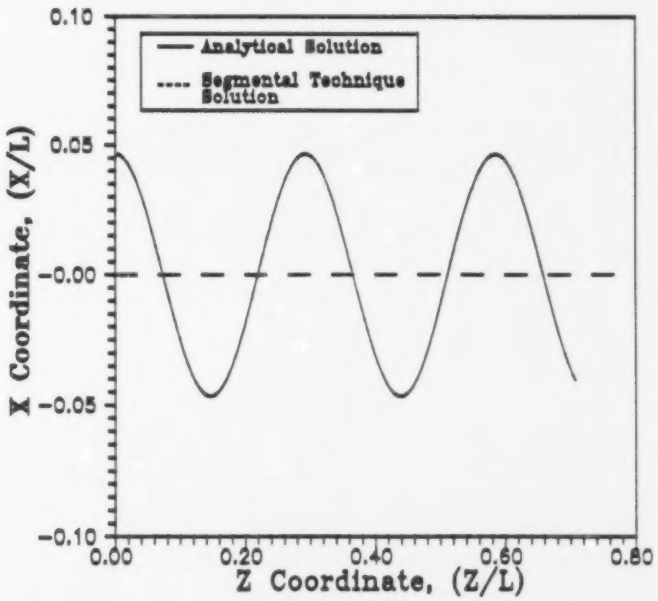

Figure 4.2a: Geometry of Deformed Helix - ZX Plane (500 Segments)
M_z=200 Nm, α=45°

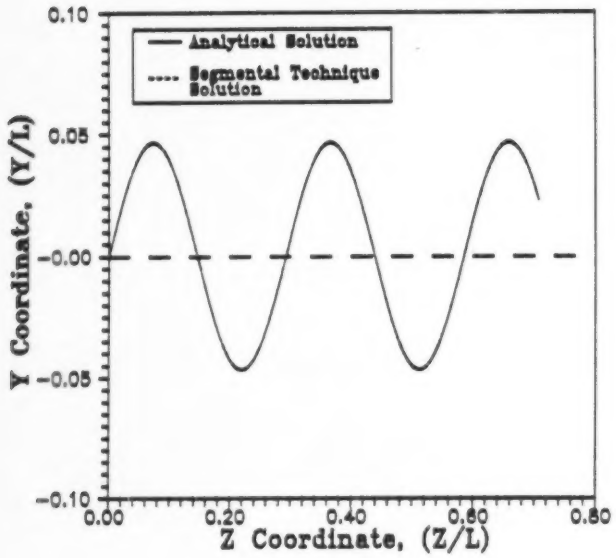

Figure 4.2b: Geometry of Deformed Helix - ZY Plane (500 Segments)
M_z=200 Nm, α=45°

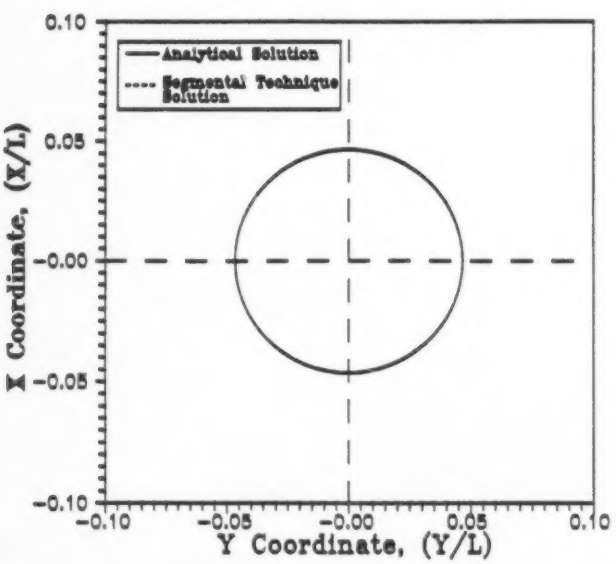

Figure 4.2c: Geometry of Deformed Helix - YX Plane (500 Segments)
M_z=200 Nm, α=45°

Figures (4.3a) - (4.3c) show the geometry obtained for the same problem when only 20 segments are used. Although the figures show kinks in the solution, this is because these figures are merely a plot of the endpoints of the segments joined by straight lines. The actual solution delivered by the segmental technique is continuous, but the curves as shown are sufficient to show there is poor agreement between the two solutions. With too few segments being used, each segment undergoes a sufficiently large deformation to cause a breakdown in the assumption that only small deformations occur over each individual segment. As a direct result the equations obtained for the case of small deformations are no longer applicable and inaccurate solutions are obtained.

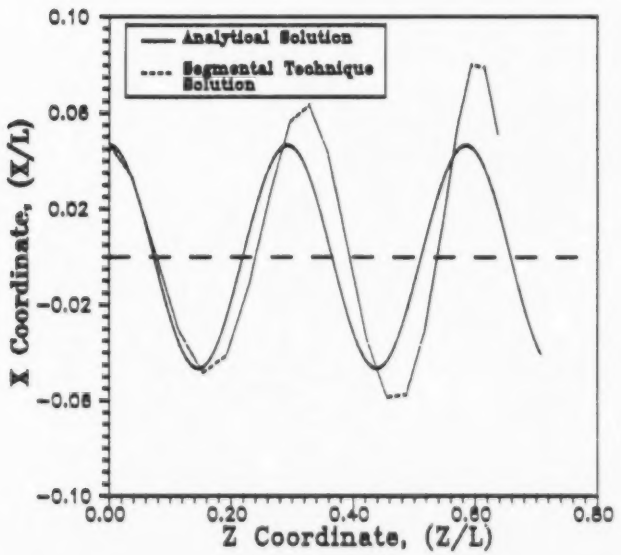

Figure 4.3a: Geometry of Deformed Helix - ZX Plane (20 Segments)
M_z=200 Nm, α=45°

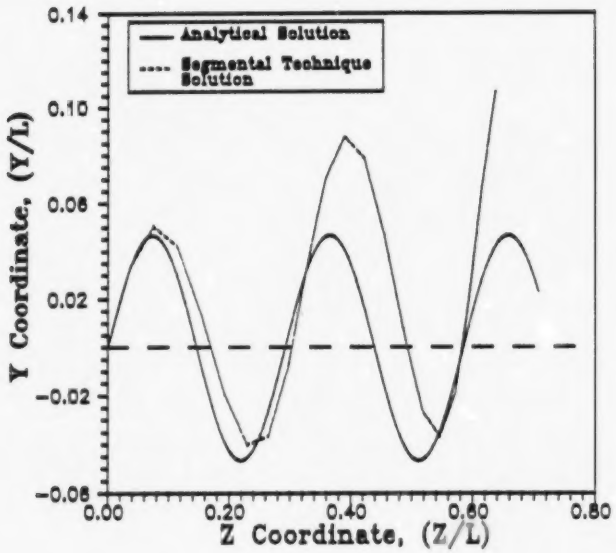

Figure 4.3b: Geometry of Deformed Helix - ZY Plane (20 Segments)
M_z=200 Nm, α=45°

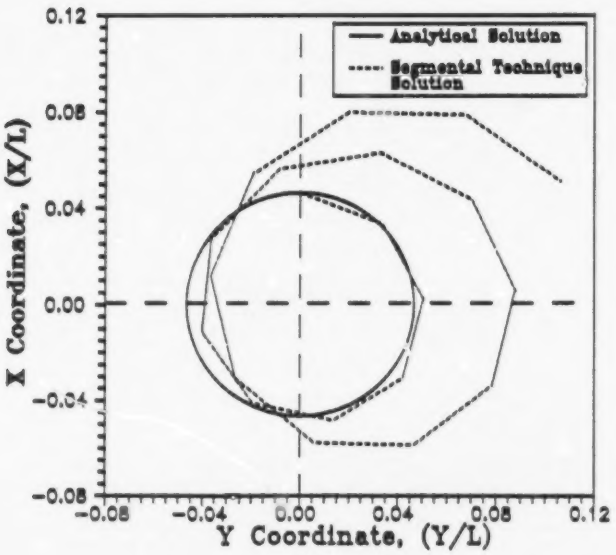

Figure 4.3c: Geometry of Deformed Helix - YX Plane (20 Segments)
M_z=200 Nm, α=45°

To further verify the results obtained with the segmental solution, there are other conditions besides geometry which must be satisfied. One such condition is that the deformed rod must be in equilibrium. Table 4.2 shows the equilibrium results for the segmental solutions obtained with an increasing number of segments. Force equilibrium for these solutions is automatically satisfied in all cases since no external forces act on the rod. The values shown in Table 4.2 are the moment equilibria taken about the global $\underline{E}_1$, $\underline{E}_2$ and $\underline{E}_3$ axes respectively. It can be seen that as the number of segments is increased, the solution obtained using the segmental technique becomes closer to satisfying overall static equilibrium. At 500 segments the magnitude of the inequality is 0.045 Nm which is 0.022% of the total applied load. When only 20 segments are used the resulting imbalance in the moment equilibrium is 28.04 Nm, or approximately 14% of the applied load. As previously mentioned, this is due to the breakdown of the assumption that only small deformations occur over each segment.

Table 4.2: Overall Equilibrium of Solutions Obtained With Segmental Technique For an Increasing Number of Segments, M_z = 200 Nm, $\alpha = 45°$

# of Segments	ΣM_1 (Nm)	ΣM_2 (Nm)	ΣM_3 (Nm)
10	-4.975870	108.70033	-59.371023
20	9.156242	1.956329	-26.430033
50	1.761369	3.971971	-2.608929
100	0.340688	1.056494	-0.332787
200	0.077438	0.267416	-0.041675
500	0.011812	0.042980	-0.002664
1000	2.909485×10^{-3}	0.010758	-3.328056×10^{-4}
2000	7.221148×10^{-4}	2.690911×10^{-3}	-4.158372×10^{-5}
5000	1.150415×10^{-4}	4.306811×10^{-4}	-2.660624×10^{-6}

A further check on the accuracy of the solutions obtained using the segmental technique can be obtained from Section 2.3. It was determined from (2.74) that for the particular constitutive relationship being used, the twist per unit length, κ, remains constant along the rod for any deformation. If no end moments are applied along the axis of the rod then there will be no twist at any point throughout the rod. If the moment applied at the start of the rod has a component along the rod's axis (M_1 in the $\underline{e}_1$ direction) then the twist per unit length κ will be given by

$$\kappa = \frac{M_1}{GJ} \tag{4.13}$$

which will be constant along the length of the rod. This can provide a further check on the accuracy of the solution obtained with the segmental technique. Figure 4.4 shows κ as a function of arc length obtained using both 20 and 500 segments. From Figure 4.4, κ remains constant along the rod when 500 segments are used with a maximum change from the initial value, which is the exact value, of only -0.004%. When only 20 segments are used, κ varies considerably along the rod with a maximum variation of 53.2% from the initial value of 15.879 m^{-1}.

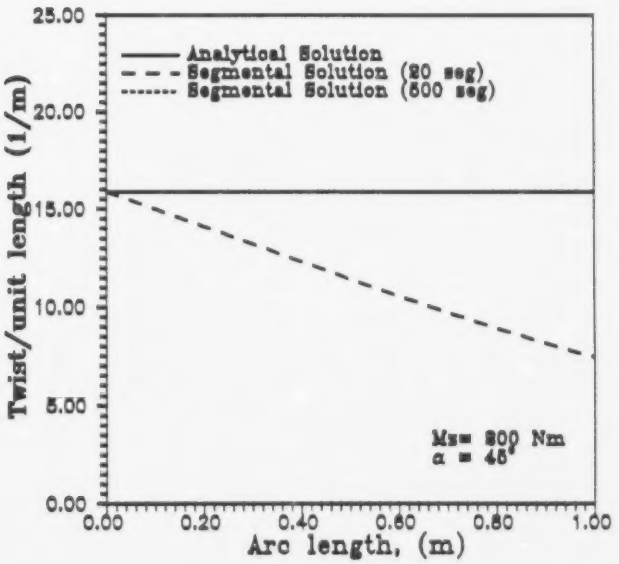

Figure 4.4: Twist Per Unit Length Along Rod (M_z = 200 Nm, α = 45°)

A further check on the accuracy of the results obtained using the segmental technique can be obtained from the derivation in Section 2.2 which provides a first integral of the equations of equilibrium. Equation (2.60) states that this integral will be constant along the rod for any deformation. This then provides another method to check the validity of the results obtained with the segmental technique. This integral can be determined at various points along the rod (at the start of each segment for example) for the current problem being considered. Figure 4.5 shows the results obtained with both 20 and 500 segments. The energy integral using 500 segments remains constant along the rod with a maximum deviation of only 0.0037% from the initial value. When 20 segments are used the maximum change from the initial value is 34.82%.

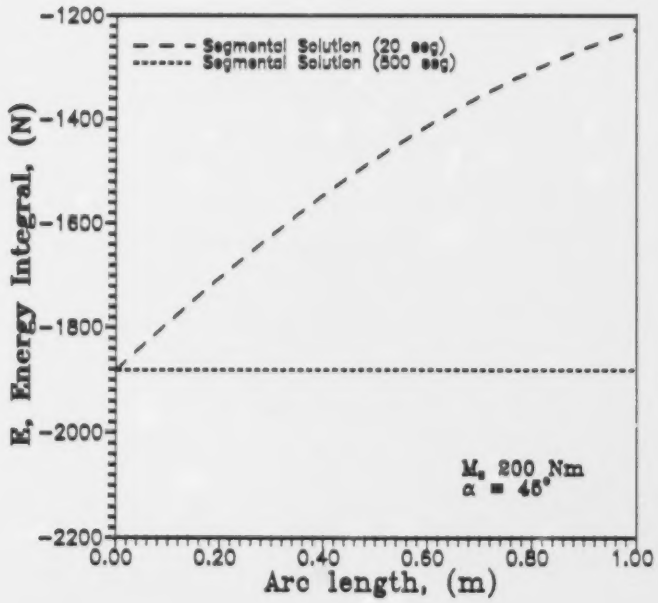

Figure 4.5: Energy Integral Evaluated Along Rod (M_z = 200 Nm, α = 45°)

These results all demonstrate that the segmental technique gives accurate solutions provided enough segments are used. 500 segments was found to give acceptable results for this particular problem. However, the number of segments required will change from problem to problem depending upon the total amount of deformation as well as the relative amounts of deformation due to either bending or twisting. To demonstrate this consider the same problem of a rod being twisted into a helical spiral by a 200 Nm axial moment and no axial force but let the pitch angle be changed from 45 to 75 degrees. This change will result in a larger portion of the applied moment producing a torsional deformation and a smaller amount of deformation due to bending. Table 4.3 shows the geometry obtained at the end of the rod using the segmental technique with a varying number of segments as well as the exact analytical solution for comparison. Table 4.4 shows the overall equilibrium results of the deformed rod for an increasing number of segments. A comparison of Tables 4.1 through 4.4 shows that to obtain a similar level of accuracy, fewer segments are required for the case where α=75°. Both problems have the same applied moment, but there is a difference in the amount of total deflection as well as the relative amounts of deflection due to both bending and twisting.

Table 4.3: Geometry at the End of a Deformed Helix, M_z=200 Nm, α=75°

# of Segments	X/L	Y/L	Z/L	$e_1(3)$
10	-0.019359	0.029804	0.985542	0.939203
20	-0.015365	0.012788	0.971498	0.964324
50	-0.014834	0.009081	0.966983	0.966041
100	-0.014794	0.008618	0.966206	0.965987
200	-0.014786	0.008510	0.965998	0.965945
500	-0.014785	0.008481	0.965938	0.965929
1000	-0.014785	0.008477	0.965929	0.965927
2000	-0.014785	0.008476	0.965927	0.965926
5000	-0.014785	0.008475	0.965926	0.965926
Analytical Result	-0.014785	0.008475	0.965926	0.965926

Table 4.4: Overall Equilibrium of Solutions Obtained With Segmental Technique For an Increasing Number of Segments, M_z = 200 Nm, α = 75°

# of Segments	ΣM_1 (Nm)	ΣM_2 (Nm)	ΣM_3 (Nm)
10	5.914040	8.978177	-13.386057
20	0.541926	1.822054	-1.370837
50	0.078500	0.287259	-0.088305
100	0.019465	0.071980	-0.011111
200	0.004840	0.018018	-0.001392
500	7.711459×10^{-4}	2.884684×10^{-3}	-8.910601×10^{-5}
1000	1.924510×10^{-4}	7.212946×10^{-4}	-1.113825×10^{-5}
2000	4.807203×10^{-5}	1.803375×10^{-4}	-1.392250×10^{-6}
5000	7.687238×10^{-6}	2.885526×10^{-5}	-8.901731×10^{-8}

With 500 segments the magnitude of the error in equilibrium for the α=45° problem was 0.0223% of the applied load. For α=75°, the error in equilibrium was 0.0094% of the same applied load when only 200 segments were used. These results demonstrate that the number of segments required to obtain a solution with a specified level of accuracy is very dependent upon the particular problem being solved.

To further illustrate this point, consider the case where α=5° with the applied loads remaining the same. The equilibrium results for the solutions obtained with the segmental technique are shown in Table 4.5.

Table 4.5: Overall Equilibrium of Solutions Obtained With Segmental Technique For an Increasing Number of Segments, M_z = 200 Nm, α = 5°

# of Segments	ΣM_1 (Nm)	ΣM_2 (Nm)	ΣM_3 (Nm)
10	25.375370	-4.614018	-1.361059
20	2.792111	4.764537	-0.518344
50	0.763758	1.121524	-0.136011
100	0.143442	0.348896	-0.019656
200	0.029388	0.091114	-0.002497
500	4.209184×10^{-3}	0.0147771	-1.597010×10^{-4}
1000	1.018401×10^{-3}	3.703278×10^{-3}	-1.993534×10^{-5}
2000	2.507281×10^{-4}	9.269352×10^{-4}	-2.489877×10^{-6}
5000	3.976388×10^{-5}	1.484070×10^{-4}	-1.593085×10^{-7}

For this case the magnitude of the error in equilibrium is 0.0077% of the applied load with 500 segments being used. This is smaller than the equilibrium error with 500

segments in the first case when α=45°. For the case of α=5° the deformation due to bending is increased and the deformation due to torsion is reduced. This is the opposite effect of increasing α from 45° to 75°, but in both cases the number of segments required to achieve a similar level of accuracy has been reduced.

These results all serve to demonstrate that the number of segments required to achieve a desired level of accuracy is very problem specific. Thus when solving problems for which the solution is not known *a priori*, it is necessary to determine if equilibrium is satisfied for every solution obtained to ensure that the solution is acceptable. It would also be prudent to check both the energy integral and twist per unit length for uniformity along the rod which would indicate a computed solution consistent with the known properties of the theory.

4.1.2 Helix with Axial Forces

The previous problems considered were all ones which included moments but no axial forces. To verify the accuracy of the segmental technique for problems in which forces are involved, the previous problem will be modified by adding an arbitrary axial tension of 100 N to the rod and again letting α=45°. To compute the radius of the helix and the twist per unit length, equations (2.81b), (2.81c) and (2.85) give

$$\begin{aligned} M_z &= GJ\kappa \sin\alpha + \frac{EI}{R}\cos^3\alpha, \\ M_\theta &= FR = GJ\kappa\cos\alpha - \frac{EI}{R}\cos^2\alpha \sin\alpha, \end{aligned} \tag{4.14}$$

where M_z, F and α are specified. This is a system of two equations for the two unknowns R and κ. Eliminating κ from (4.14) and solving for the radius results in a quadratic equation which gives the radius R as

$$R = \frac{\cos\alpha}{2F\sin\alpha}\left(M_z \pm \sqrt{M_z^2 - 4EIF\sin\alpha}\right). \qquad (4.15)$$

The corresponding value for κ can be obtained by substitution of R into (4.14). Therefore, from (4.15), for given values of M_z, F and α there may be two solutions for the radius and a corresponding κ or there may be no solution if the square root term in (4.15) is negative. This was not the case when there was no axial force. It should also be noted that the above solution is undefined when F=0 or when α=0. However, when F=0, κ and R are given by (2.86) and (2.87) respectively. When α=0, the rod remains straight (infinite radius) as there is no component of the applied moment to cause a bending deformation.

For the current problem, (4.14) and (4.15) give two values for R and the corresponding κ, namely

$$(R)_1 = 0.04769610 \text{ m} \qquad (\kappa)_1 = 16.25726757 \text{ m}^{-1},$$

$$(R)_2 = 1.95230390 \text{ m} \qquad (\kappa)_2 = 31.37851470 \text{ m}^{-1}.$$

From the first set of values, M_θ, which depends on both the axial force and the radius, is 4.769610 Nm. Then with the moments, forces and geometry at the start of the rod specified, the corresponding values at the start of the first segment are determined as before with equations (4.6) and (4.8)-(4.12). Figures 4.6a - 4.6c show the geometry of the resulting solution obtained with 500 segments as well as the exact solution.

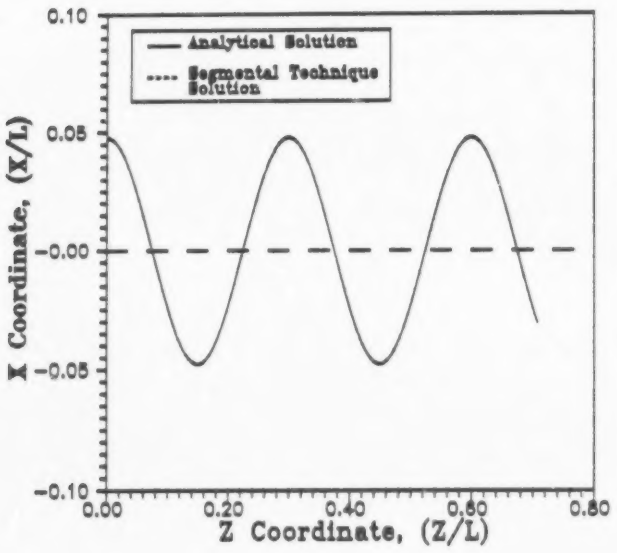

Figure 4.6a: Geometry of Deformed Helix - ZX Plane (500 Segments)
M_z = 200 Nm, F_z = 100 N, α = 45°, R = 0.0476961 m

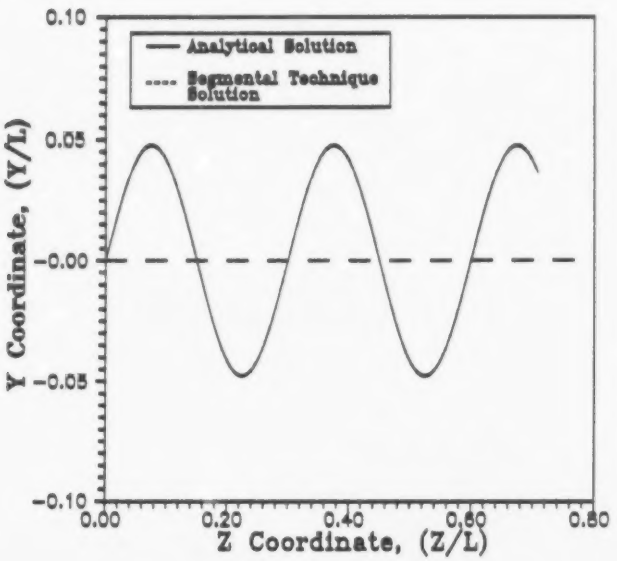

Figure 4.6b: Geometry of Deformed Helix - ZY Plane (500 Segments)
M_z = 200 Nm, F_z = 100 N, α = 45°, R = 0.0476961 m

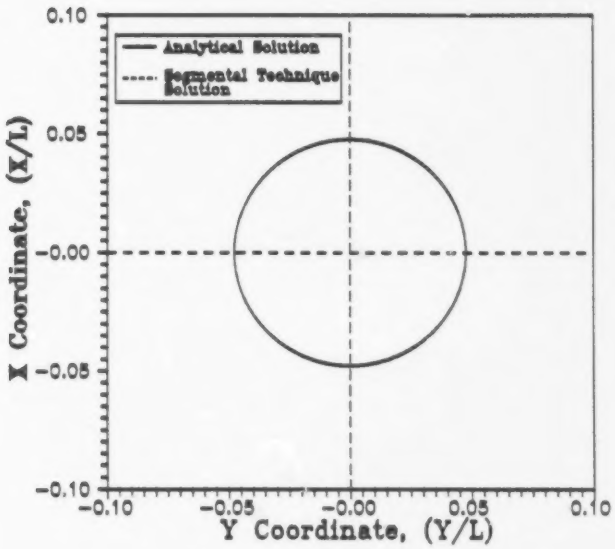

Figure 4.6c: Geometry of Deformed Helix - YX Plane (500 Segments)
M_z = 200 Nm, F_z = 100 N, α = 45°, R = 0.0476961 m

These figures show close agreement between the geometries of the two solutions. This is an indication that 500 segments is sufficient for this problem. Figures 4.7 and 4.8 show κ and the energy integral along the rod respectively. There is a 0.004% change in κ and a 0.003% change in the energy integral. As well, the magnitude of the resulting imbalance in equilibrium of the segmental solution was 4.09×10^{-14} N for the forces and 0.0407 Nm for the moments. These results all indicate that the solution computed by the segmental technique is acceptable.

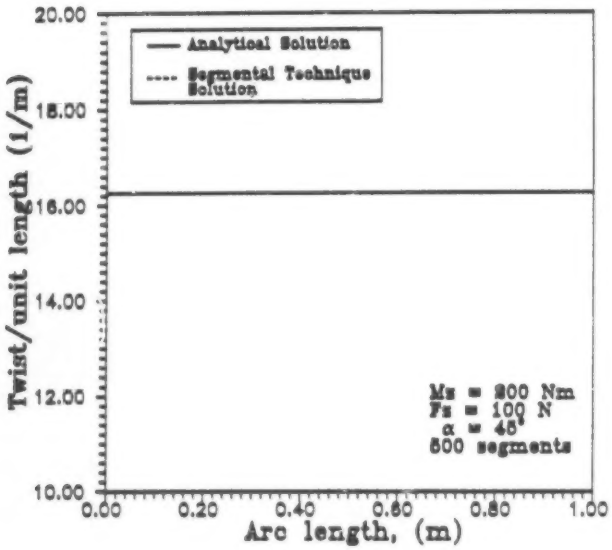

Figure 4.7: Twist Per Unit Length Along Rod - (500 Segments)
M_z = 200 Nm, F_z = 100 N, α = 45°, R = 0.0476961 m

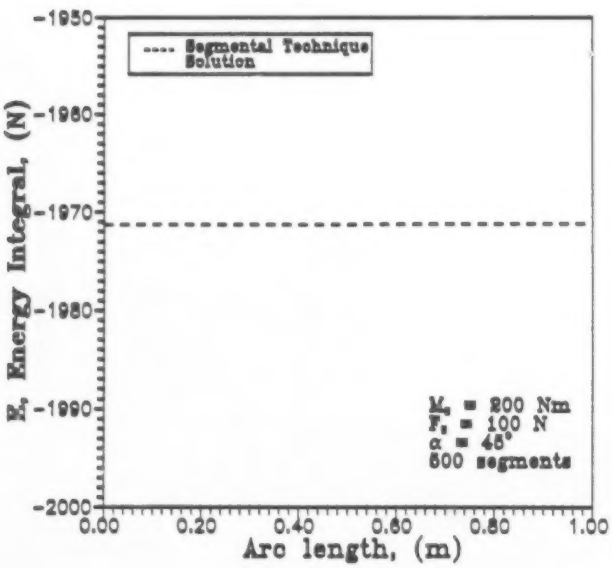

Figure 4.8: Energy Integral Evaluated Along Rod - (500 Segments)
M_z = 200 Nm, F_z = 100 N, α = 45°, R = 0.0476961 m

Using the second set of R and κ determined for this problem, M_0 was found to be 195.230390 Nm. In this case the computed radius is much larger than before. With the rod having the same overall length as before, the rod is unable to complete a full helix. The geometries obtained with the segmental technique using this initial value for M_0 and 500 segments are shown in Figures 4.9a - 4.9c. Again from these figures it is evident that there is close agreement between the exact analytical solution and the solution delivered by the segmental technique. As a further check Figures 4.10 and 4.11 show the twist per unit length and energy integral for this problem. These results also show close agreement with the exact solution.

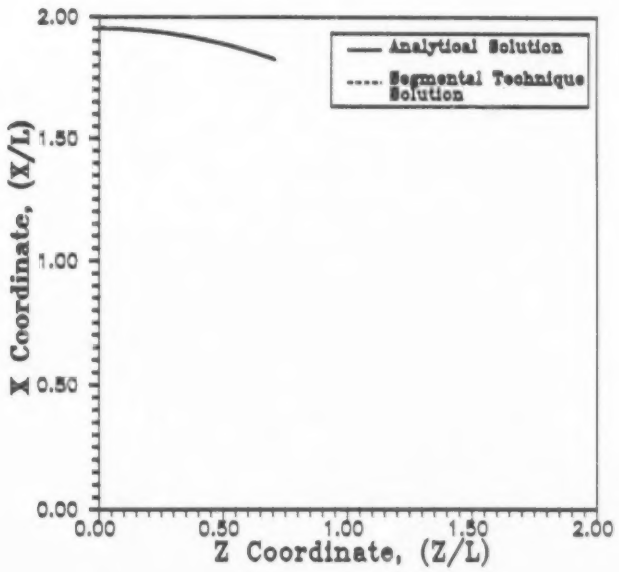

Figure 4.9a: Geometry of Deformed Helix - ZX Plane (500 Segments)
M_z = 200 Nm, F_z = 100 N, α = 45°, R = 1.9523039 m

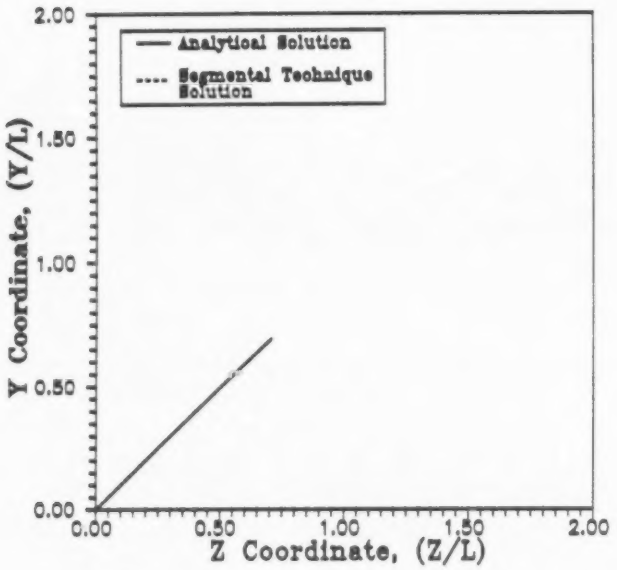

Figure 4.9b: Geometry of Deformed Helix - ZY Plane (500 Segments)
M_z = 200 Nm, F_z = 100 N, α = 45°, R = 1.9523039 m

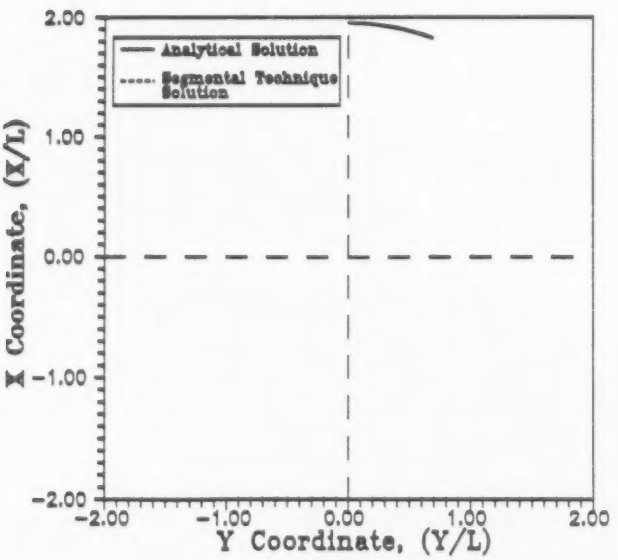

Figure 4.9c: Geometry of Deformed Helix - YX Plane (500 Segments)
M_z = 200 Nm, F_z = 100 N, α = 45°, R = 1.9523039 m

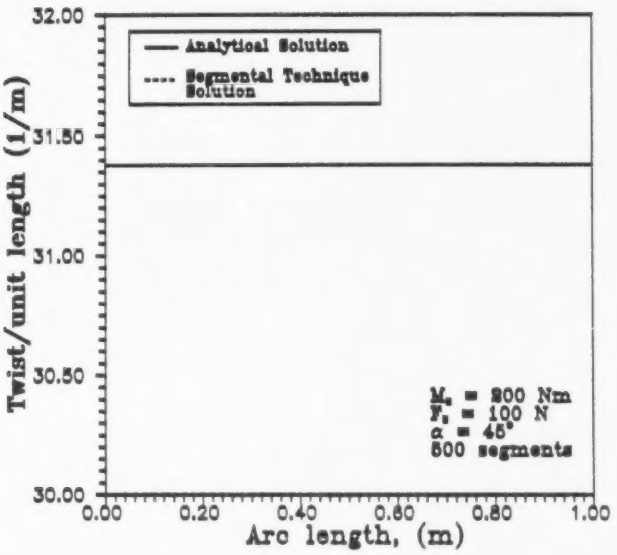

Figure 4.10: Twist per Unit Length Along Rod - (500 Segments)
M_z = 200 Nm, F_z = 100 N, α = 45°, R = 1.9523039 m

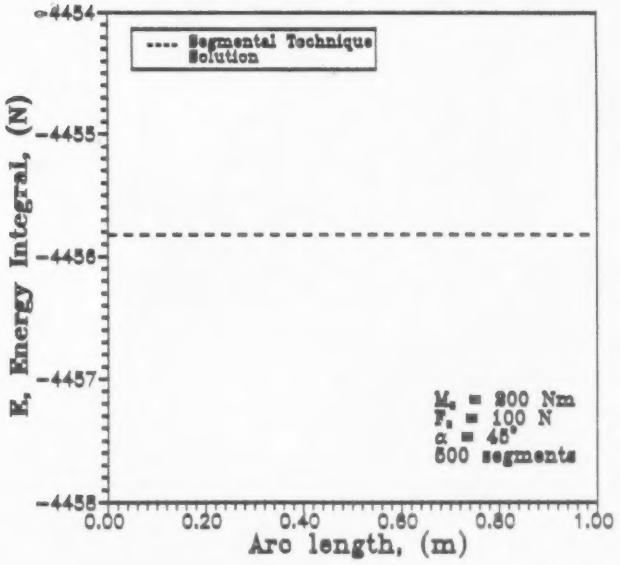

Figure 4.11: Energy Integral Evaluated Along Rod - (500 Segments)
M_z = 200 Nm, F_z = 100 N, α = 45°, R = 1.9523039 m

The results for the current problem being investigated show that two equilibrium configurations in the form of helices were obtained for the same specified initial conditions of force, moment and pitch angle α. This ability of the segmental technique to analyse multiple equilibrium configurations for a given problem by varying initial conditions has been demonstrated by Tam [13] for planar elastica problems.

4.2 SHOOTING PROBLEM

In the previous sections the segmental technique was used to generate the deformed shaped of the rod as well as the forces and moments which act along the rod. The results obtained were compared to the exact analytical solution to test the validity of the solution delivered by the segmental technique. The solutions thus obtained showed excellent agreement with the analytical solutions provided a sufficient number of segments were used. These results, however, were based on a complete knowledge of the conditions at the start of the rod. There were no boundary conditions at the end of the rod which needed to be satisfied. This section presents the problem as one which has a single unknown at the start of the rod to demonstrate how the shooting procedure, presented in Section 3.4, is used to solve such problems.

Consider the previous problem where the rod is to be twisted into a helical spiral by a specified axial moment and force. This time, however, the pitch angle at the start of the rod is not specified but rather the deformed helix is specified to have a known axial length z_0. The major difference between this problem and the problem in the previous section is that previously the initial pitch angle α was specified *a priori*. This time, the pitch angle at the start of the rod is not known *a priori*, but must be chosen

such that the resulting helix meets the specified boundary condition, namely $z(L) = z_0$. This can be considered as a problem with one unknown parameter since in this case the conditions (forces, moments and geometry) at the start of the rod are a function of the pitch angle only (with M_z and F_z specified).

It should be noted here that an exact analytical solution for this problem is available to calculate the appropriate pitch angle α (equations (4.2) and (4.5)). To demonstrate the shooting procedure, however, it will be assumed that such analytical information is not available, as would be the case in most practical problems. In what follows, however, it will be assumed that the deformed configuration of the rod is in all cases a helix with radius R and pitch angle α. The forces and moments at the start of the rod, which are functions of α only (with M_z and F_z specified), will be chosen such that the resulting shape is a helix in accordance with (2.81). In general, this *a priori* knowledge will not be available. As a result there would be more unknowns at the start of the rod since the helical deformed shaped would not be known beforehand and the relationships between the moments, forces, radius R and α would not be available. As well, the boundary conditions at the end of the segment would become correspondingly more complicated. However, for the purpose of demonstrating the shooting procedure, it will be assumed that such analytical information is available so that the problem can be presented as one with a single unknown variable (α) at the start of the rod and with a single corresponding known boundary condition at the end of the rod ($z(L) = z_0$). The only exception to this assumption is that the solution relating the pitch angle α and the axial length z is not known *a priori*.

Consider the previous problem where the same rod is to be twisted into a helix by an axial moment of 200 Nm and an axial tension of 100 N. As well the axial length of the deformed helix is specified to be 0.6m. To start the segmental procedure an initial estimate of the unknown pitch angle must be made. This initial guess is then used to calculate the conditions at the start of the rod as before. The segmental solution then solves the entire rod exactly as before. The axial length delivered by the segmental solution will be a function (not analytical) of the initial estimate of α. To illustrate this point, Figure 4.12 shows the axial length of the resulting helix as a function of the initial pitch angle α for the segmental technique using 500 segments.

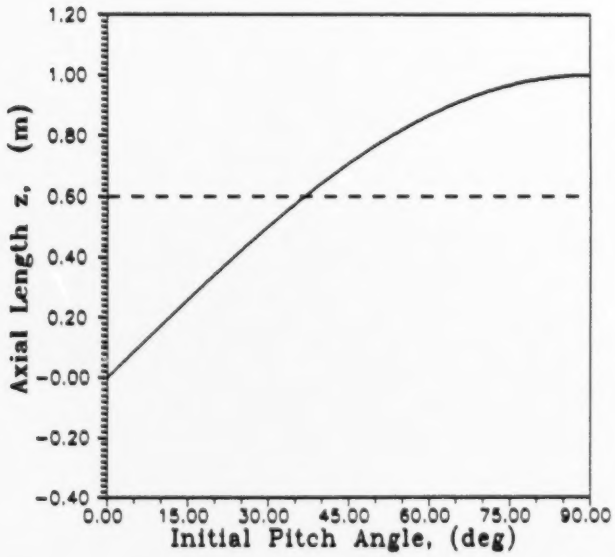

Figure 4.12: Axial Length z as a Function of Initial Pitch Angle α

This figure was generated by inputing initial values of α from 0 to 90° in increments of 0.5° into the segmental technique and calculating the resultant axial length. At this point no shooting has been involved. The purpose of this procedure is to demonstrate the functional relationship between axial length z and initial pitch angle α. From this figure it can be seen that the axial length is 0.6m when the initial pitch angle is approximately 37°. Also, since α can only take on values from 0 to 90° from physical considerations, this figure also shows that this is the only pitch angle which satisfies the required boundary condition. This value will not be known *a priori*, however, and the initial estimate may or may not be close to this value. For the purpose of illustration, assume that the initial estimate of the pitch angle is 10°. The segmental technique returns an axial length of 0.1664 m. This does not agree with the specified boundary condition of 0.6m. Therefore the segmental technique calculates an approximate derivative $dz/d\alpha$ in order to use the Newton Raphson false position method. This approximate derivative requires another initial guess close to the initial α to perform the backward substitution process. Hence two estimates of the initial pitch angle are required to start the technique. In general, if there are N unknowns at the start of the rod then 2N initial estimates of the unknowns are required. To determine the partial derivatives, N passes of the segmental approach are required. Thus each iteration requires N+1 passes of the segmental approach. Based on the axial length returned by the initial estimate of 10° and the approximated derivative at this point, the Newton Raphson method returns an improved estimate of 35.06°. This new estimate of α then returns an axial length of 0.5726 m. This procedure is repeated until the axial length returned by the segmental technique converges to the required boundary condition within

some set tolerance. Table 4.6 shows the convergence behavior for this problem.

Table 4.6: Convergence Behavior of One Variable Shooting Problem

Iteration #	Pitch Angle α, (°)	Axial Length z, (m)	Convergence (z_0-z)
1	10	0.16646864915426	4.335314×10^{-1}
2	35.062553337435	0.57264143331626	2.735857×10^{-2}
3	36.750690907168	0.59697891778891	3.021082×10^{-3}
4	36.960244297435	0.59996428828048	3.571172×10^{-5}
5	36.962751025467	0.59999995144569	4.855431×10^{-8}
6	36.962754438301	0.59999999999922	7.842615×10^{-13}

Table 4.6 shows that segmental shooting technique converges quickly and monotonically for this problem. This is to be expected since Figure 4.12 shows that the function is well behaved. In some problems, however, these functions may be quite complex with steep gradients near the points of interest [13]. In such cases, especially for problems with two or more unknowns at the start of the rod, initial estimates close to the actual values are required. Relaxation factors may also be used to improve convergence.

CHAPTER

FIVE

CONCLUSIONS

5.1 SUMMARY

The objective of the present study was to develop a numerical procedure to analyse problems involving large three dimensional deflections of thin flexible rods. The equations that describe such deformations are highly nonlinear and difficult to solve analytically. This difficulty is further compounded by the wide variety of boundary conditions which may be involved. As a result, numerical procedures are usually required to obtain approximate solutions to such problems. This thesis presents a new approach to this problem.

The numerical procedure developed in the foregoing is based on the *segmental shooting technique*, a numerical method previously found to be successful for planar elastica problems. The major advantage of this technique is that the nonlinearity of the problem is avoided by dividing the rod under consideration into a large number of shorter segments, each of which undergoes only small deformations relative to neighboring segments. The equations describing the deformations of these individual segments can therefore be linearized and solved by standard techniques. The individual segments are assembled together, maintaining compatibility and continuity, to form the complete rod. In this way, the nonlinearity of the problem is avoided by solving a sequence of linear problems. In doing so, the original boundary value problem is converted into an initial value problem. A Newton Raphson false position technique is

then used to ensure that the appropriate boundary conditions are satisfied.

The segmental shooting technique has several advantages over other techniques. Since each segment of the rod is analyzed separately, large computer memory space is not required as with the finite element method. As well, incremental loading is not required to handle large deflections, resulting in a much faster solution. For example, the solutions obtained in the previous chapter using 500 segments were all done on an IBM 80486/487 personal computer in under 5 seconds each. The segmental technique, as was noted previously [13], is well suited to finding multiple equilibrium configurations when they exist.

The major drawback with this technique is that the false position iterative procedure which allows the boundary conditions to be satisfied is susceptible to numerical problems due to the numerical differentiation involved in estimating partial derivatives of complex functions. As well, initial estimates of the unknown parameters close to the actual values are usually required to ensure convergence of the solution. It has been previous experience that when three boundary conditions (the maximum number for planar problems) were required for a given problem the convergence behavior of the solution became much slower than for problems with one or two boundary conditions. Three dimensional problems could easily have more than three boundary conditions which need to be satisfied. The convergence behavior for such problems will likely become worse. This requires further investigation.

The most significant difference between planar and three dimensional rod problems is that the twist along the rod couples the two transverse bending components. In planar problems no twisting occurs and one equation is sufficient to describe the

deformation. For three dimensional problems, there are three differential equations, coupled by the twist, which describe the deformation of a rod segment. For the special case where the rod is initially straight and of circular cross section (the case investigated in this thesis) the bending components may be uncoupled from the twist resulting in two differential equations to be solved for the transverse deflections. The third equation for the twist can then be solved separately.

The computer program developed to implement this technique was used to solve the problem of an initially straight rod with circular cross section twisted into a helical spiral by axially applied end moments and forces. This problem has a well known analytical solution and served to verify the results obtained using the segmental technique. The resulting geometry, equilibrium results, a first integral of the equilibrium equations and a condition imposed on the solution from constitutive assumptions were all used to determine the validity of the numerical solution. In all cases it was found that there was close agreement between the analytical and segmental solutions provided that a sufficient number of segments were used. The possibility of obtaining multiple helices for specified applied loadings was noted and these multiple equilibrium configurations were found easily using the segmental technique.

5.2 FUTURE WORK

The present work considers only the special case of a rod with circular cross section which is initially straight, inextensible, and has a quadratic strain energy function. To allow this procedure to be applied to a wider variety of practical engineering

problems the procedure should be modified to consider rods with different cross sections as well as rods with initial curvatures and pre-twisted rods. Extensibility should also be considered since this may be an important consideration in some problems. Major modifications to the technique may, in the future, allow it to be applied to materials with different constitutive relationships as well as to a dynamical analysis of rod structures.

REFERENCES

[1] Love, A.E.H. *A Treatise on the Mathematical Theory of Elasticity*, Dover Publications, 4th edition, 1972

[2] Landau, L.D. and Lifshitz, E.M. *Theory of Elasticity*, Pergamon Press, 2nd edition, 1970

[3] Steigmann, D.J. and Faulkner, M.G. "Variational Theory For Spatial Rods", *Journal of Elasticity*, accepted for publication, 1992

[4] Surana, K.S. and Sorem, R.M. "Geometrically Nonlinear Formulation for Three Dimensional Curved Beam Elements with Large Rotations", *International Journal for Numerical Methods in Engineering*, Vol. 28, 1989, pp. 43-73.

[5] Frisch-Fay. *Flexible Bars*, Butterworths, London, 1962

[6] Wang, C.Y. "A Critical Review of The Heavy Elastica", *International Journal of Mechanical Sciences*, Vol. 28, No. 8, 1986, pp. 549-559.

[7] Faulkner, M.G. and Stredulinsky, D.C. "Nonlinear Bending of Inextensible Thin Rods Under Distributed and Concentrated Loads", *Transactions of the CSME*, Vol. 4, No. 2, 1976-1977, pp. 77-81.

[8] El-Rayes, K. *Numerical Analysis of Orthodontic Appliances*, M.Sc. Thesis, University of Alberta, 1989

[9] Lipsett, A.W., Faulkner, M.G. and El-Rayes, K. "Large Deformation Analysis of Orthodontic Appliances", *Journal of Biomechanical Engineering*, Vol. 112, 1990, pp. 29-37.

REFERENCES (continued)

[10] Faulkner, M.G., Lipsett, A.W. and Tam, V. "On The Use of a Segmental Shooting Technique for Multiple Solutions of Planar Elastica Problems", submitted to *Comput. Meths. Appl. Mech. Engrg.*, June 1991

[11] Gurtin, M.E. *An Introduction to Continuum Mechanics*, Academic Press Inc., 1981

[12] Bliss, G.A. *Lectures on the Calculus of Variations*, University of Chicago Press, Chicago ,1946

[13] Tam, V. *Multiple Solutions of Plane Elasticae*, M.Sc. Thesis, University of Alberta, 1991

APPENDIX

A

Dimensional Analysis of Equilibrium Equation

A dimensional analysis was performed on the equilibrium equation given in (3.18). This was done to ensure that the proper terms are retained when the assumption that only small deflections occur over a given segment was applied. The relevant terms were expressed relative to some reference values and ratios of small to large values (order ε) were obtained. The analysis was performed to determine which terms were more than order one in ε and these were subsequently neglected.

GOVERNING EQUATIONS

The pertinent equations from Chapter 3 are repeated here for convenience.

Equilibrium

$$\underline{F}' + \underline{b} = \underline{0} \tag{A.1}$$

$$\underline{M}' = \underline{F} \times \underline{t} \tag{A.2}$$

Constitutive Relationship

$$\underline{M} = EI\underline{t} \times \underline{t}' + GJ\kappa\underline{t} \tag{A.3}$$

Differentiating (A.3) with respect to arc length gives

$$\underline{M}' = EI\underline{t} \times \underline{t}'' + GJ\kappa'\underline{t} + GJ\kappa\underline{t}'. \tag{A.4}$$

Now define

$$\underline{f} = \frac{\underline{F}}{F_{ref}}, \quad \underline{m} = \frac{\underline{M}}{M_{ref}}, \quad \rho = \frac{s}{L}, \quad K = \frac{\kappa}{K_{ref}}. \tag{A.5}$$

Here F_{ref}, M_{ref} and K_{ref} are reference magnitudes of the force, moment and twist per unit length respectively. These will be used later to determine which quantities are "small". s is the arc length parameter and L is the length of a segment. ρ is therefore the dimensionless arc length parameter. Also, from equation (3.17),

$$\kappa = \Phi_0 + k \tag{A.6}$$

so

$$K = \frac{\Phi_0}{K_{ref}} + \frac{k_{ref}}{K_{ref}}\Omega, \quad \Omega = \frac{k}{k_{ref}}. \tag{A.7}$$

As well from (3.7),

$$\mathbf{t} = \mathbf{t}^0 + \mathbf{u}', \tag{A.8}$$

so that

$$\mathbf{t}' = \mathbf{u}'', \qquad \mathbf{t}'' = \mathbf{u}'''. \tag{A.9}$$

Also define

$$\underline{\mathbf{U}} = \frac{\mathbf{u}}{U_{ref}}, \tag{A.10}$$

where U_{ref} is a reference deflection, then

$$\mathbf{u}' = \frac{U_{ref}}{L}\dot{\underline{\mathbf{U}}}, \qquad \mathbf{u}'' = \frac{U_{ref}}{L^2}\ddot{\underline{\mathbf{U}}}, \qquad \mathbf{u}''' = \frac{U_{ref}}{L^3}\tilde{\underline{\mathbf{U}}}, \tag{A.11}$$

where the dot notation indicates differentiation with respect to ρ, the dimensionless arc length defined in (A.5).

Using the parameters defined above, (A.2) becomes

$$\frac{d\mathbf{M}}{ds} = \mathbf{F}\times\mathbf{t}^0 + \mathbf{F}\times\mathbf{u}', \tag{A.12}$$

or

$$\frac{M_{ref}}{L}\frac{d\mathbf{m}}{d\rho} = F_{ref}\mathbf{f}\times\mathbf{t}^0 + F_{ref}\mathbf{f}\times\frac{U_{ref}}{L}\dot{\underline{\mathbf{U}}},$$

$$\frac{M_{ref}}{L}\dot{\mathbf{m}} = F_{ref}\mathbf{f}\times\mathbf{t}^0 + \frac{F_{ref}U_{ref}}{L}\mathbf{f}\times\dot{\underline{\mathbf{U}}}. \tag{A.13}$$

Equation (A.4) becomes

$$\frac{M_{ref}}{L}\dot{\underline{m}} - EI\left(\underline{t}^0 + \underline{u}'\right)\times\underline{u}''' + GJk'\left(\underline{t}^0 + \underline{u}'\right) + GJ\left(\Phi_0 + k\right)\underline{u}''$$

$$- EI\left(\underline{t}^0 + \frac{U_{ref}}{L}\dot{\underline{U}}\right)\times\frac{U_{ref}}{L^3}\ddot{\underline{U}} + GJ\frac{k_{ref}}{L}\dot{\Omega}\left(\underline{t}^0 + \frac{U_{ref}}{L}\dot{\underline{U}}\right)$$

$$+ GJ\left(\Phi_0 + \Omega k_{ref}\right)\frac{U_{ref}}{L^2}\ddot{\underline{U}}$$

$$- \frac{EI}{L^2}\frac{U_{ref}}{L}\underline{t}^0\times\ddot{\underline{U}} + \frac{EI}{L^2}\left(\frac{U_{ref}}{L}\right)^2\dot{\underline{U}}\times\ddot{\underline{U}} + \frac{GJk_{ref}}{L}\dot{\Omega}\underline{t}^0 \qquad (A.14)$$

$$+ \frac{GJk_{ref}}{L}\frac{U_{ref}}{L}\dot{\Omega}\dot{\underline{U}} + \frac{GJ\Phi_0}{L}\frac{U_{ref}}{L}\ddot{\underline{U}} + \frac{GJk_{ref}}{L}\frac{U_{ref}}{L}\Omega\ddot{\underline{U}}.$$

Equating (A.13) and (A.14) gives

$$F_{ref}\underline{f}\times\underline{t}^0 + \frac{F_{ref}U_{ref}}{L}\underline{f}\times\dot{\underline{U}} -$$

$$\frac{EI}{L^2}\frac{U_{ref}}{L}\underline{t}^0\times\ddot{\underline{U}} + \frac{EI}{L^2}\left(\frac{U_{ref}}{L}\right)^2\dot{\underline{U}}\times\ddot{\underline{U}} + \frac{GJk_{ref}}{L}\dot{\Omega}\underline{t}^0$$

$$+ \frac{GJk_{ref}}{L}\frac{U_{ref}}{L}\dot{\Omega}\dot{\underline{U}} + \frac{GJ\Phi_0}{L}\frac{U_{ref}}{L}\ddot{\underline{U}} + \frac{GJk_{ref}}{L}\frac{U_{ref}}{L}\Omega\ddot{\underline{U}},$$

and dividing through by F_{ref} gives

$$\underline{f}\times\underline{t}^0 + \frac{U_{ref}}{L}\underline{f}\times\dot{\underline{U}} -$$

$$\frac{EI}{F_{ref}L^2}\frac{U_{ref}}{L}\underline{t}^0\times\ddot{\underline{U}} + \frac{EI}{F_{ref}L^2}\left(\frac{U_{ref}}{L}\right)^2\dot{\underline{U}}\times\ddot{\underline{U}} + \frac{GJ}{F_{ref}L^2}k_{ref}L\dot{\Omega}\underline{t}^0 \qquad (A.15)$$

$$+\frac{GJ}{F_{ref}L^2}k_{ref}L\frac{U_{ref}}{L}\dot{\Omega}\dot{\underline{U}} + \frac{GJ}{F_{ref}L^2}\Phi_0 L\frac{U_{ref}}{L}\ddot{\underline{U}} + \frac{GJ}{F_{ref}L^2}k_{ref}L\frac{U_{ref}}{L}\Omega\ddot{\underline{U}}.$$

Consider equation (A.3) evaluated at s=0 (the start of the segment),

$$\underline{M}(0) = EI\,\underline{t}\times\underline{t}' + GJ\kappa\,\underline{t}. \qquad (A.16)$$

At s=0, $\underline{t} = \underline{t}^0$, $\underline{t}' = \underline{u}''$ and $\kappa = \Phi_0$ so (A.16) becomes

$$\underline{M}(0) = EI\,\underline{t}^0\times\underline{u}'' + GJ\Phi_0\underline{t}^0$$

$$= EI\,\underline{t}^0\times\frac{U_{ref}}{L^2}\ddot{\underline{U}} + GJ\Phi_0\underline{t}^0 \qquad (A.17)$$

$$= \frac{EI\,U_{ref}}{L^2}\underline{t}^0\times\ddot{\underline{U}} + GJ\Phi_0\underline{t}^0.$$

The magnitude of $\underline{M}(0)$ is then

$$|\underline{M}(0)| = \sqrt{\left(\frac{EI\,U_{ref}}{L^2}\right) + (GJ\Phi_0)^2}\,. \qquad (A.18)$$

Defining the quantities

$$M_{ref_1} = \frac{EI\,U_{ref}}{L^2}, \qquad (A.19)$$

$$M_{ref_2} = GJ\Phi_0, \tag{A.20}$$

equation (A.15) becomes

$$f\times t^0 + \frac{U_{ref}}{L} f\times \dot{U} =$$

$$\frac{M_{ref_1}}{F_{ref}L} t^0\times \bar{U} + \frac{M_{ref_1}}{F_{ref}L}\frac{U_{ref}}{L} \dot{U}\times \bar{U} + \frac{M_{ref_2}}{F_{ref}L}\frac{k_{ref}}{\Phi_0} \dot{\Omega} t^0 \tag{A.21}$$

$$+ \frac{M_{ref_2}}{F_{ref}L}\frac{k_{ref}}{\Phi_0}\frac{U_{ref}}{L} \dot{\Omega}\dot{U} + \frac{M_{ref_2}}{F_{ref}L}\frac{U_{ref}}{L}\ddot{U} + \frac{M_{ref_2}}{F_{ref}L}\frac{k_{ref}}{\Phi_0}\frac{U_{ref}}{L}\Omega\ddot{U}.$$

Now consider equation (A.2) evaluated at s=0 so that

$$M'(0) = F\times t^0$$

or

$$\frac{M_{ref}}{L}\dot{m} = F_{ref} f\times t^0. \tag{A.22}$$

The magnitude is then

$$\left|\frac{dM}{ds}\right| = \left|\frac{M_{ref}}{L}\dot{m}\right| = |F_{ref} f\times t^0| \tag{A.23}$$

and therefore,

$$\frac{M_{ref}}{L}|\dot{m}| = F_{ref}|f\times t^0|. \tag{A.24}$$

t^0 is a unit vector specifying the tangent direction along the rod. f is a unit vector in the direction of the internal contact force at arc length s=0. f can have any orientation (ie: independent of t^0). The orientation of f, which determines the magnitude of $f\times t^0$, will determine the magnitude of $(m)'$. Therefore we can say that

$$M_{ref} \sim F_{ref} L. \tag{A.25}$$

Using (A.25) and defining

$$\alpha = \frac{M_{ref_1}}{M_{ref}} = \frac{M_{ref_1}}{\sqrt{(M_{ref_1})^2 + (M_{ref_2})^2}}, \tag{A.26}$$

$$\beta = \frac{M_{ref_2}}{M_{ref}} = \frac{M_{ref_2}}{\sqrt{(M_{ref_1})^2 + (M_{ref_2})^2}}, \tag{A.27}$$

equation (A.21) becomes

$$\begin{aligned} \mathbf{f} \times \mathbf{t}^0 + \frac{U_{ref}}{L} \mathbf{f} \times \dot{\underline{U}} = \\ \alpha \mathbf{t}^0 \times \ddot{\underline{U}} + \alpha \frac{U_{ref}}{L} \dot{\underline{U}} \times \ddot{\underline{U}} + \beta \frac{k_{ref}}{\Phi_0} \dot{\Omega} \mathbf{t}^0 \\ + \beta \frac{k_{ref}}{\Phi_0} \frac{U_{ref}}{L} \dot{\Omega} \dot{\underline{U}} + \beta \frac{U_{ref}}{L} \ddot{\underline{U}} + \beta \frac{k_{ref}}{\Phi_0} \frac{U_{ref}}{L} \Omega \ddot{\underline{U}}. \end{aligned} \tag{A.28}$$

The terms (U_{ref}/L) and (k_{ref}/Φ_0) are assumed to be small (of order ε where $\varepsilon << 1$) when the segment being solved is sufficiently short. The other terms in (A.28) are approximately of order 1. Any terms with two or more order ε terms will be ignored as being higher order terms. The terms remaining are those shown in equation (3.18).

This same dimensional analysis was performed on the moment equation (3.30) to ensure the retention of the proper terms in equation (3.70). Again consider the

constitutive relationship

$$\underline{M} = EI\,\underline{t}\times\underline{t}' + GJ\kappa\,\underline{t} \tag{A.29}$$

and substituting for $\underline{t}$, $\underline{t}'$ and κ as before gives

$$\begin{aligned}\underline{M} = {} & EI\left(\underline{t}^0 + \underline{u}'\right)\times\underline{u}'' + GJ\left(\Phi_0 + \Omega k_{ref}\right)\left(\underline{t}^0 + \underline{u}'\right) \\ & - EI\left(\underline{t}^0 + \frac{U_{ref}}{L}\underline{\dot{U}}\right)\times\frac{U_{ref}}{L}\underline{\ddot{U}} + GJ\left(\Phi_0 + \Omega k_{ref}\right)\left(\underline{t}^0 + \frac{U_{ref}}{L}\underline{\dot{U}}\right) \\ & - \frac{EI\,U_{ref}}{L^2}\underline{t}^0\times\underline{\ddot{U}} + \frac{EI\,U_{ref}}{L^2}\frac{U_{ref}}{L}\underline{\dot{U}}\times\underline{\ddot{U}} + GJ\Phi_0\underline{t}^0 \\ & + GJ\Phi_0\frac{U_{ref}}{L}\underline{\dot{U}} + GJ\Phi_0\frac{k_{ref}}{\Phi_0}\Omega\underline{t}^0 + GJ\Phi_0\frac{k_{ref}}{\Phi_0}\frac{U_{ref}}{L}\Omega\underline{\dot{U}}.\end{aligned} \tag{A.30}$$

Using the results of (A.19) and (A.20) this becomes

$$\begin{aligned}\underline{M} = {} & M^1_{ref}\underline{t}^0\times\underline{\ddot{U}} + M^1_{ref}\frac{U_{ref}}{L}\underline{\dot{U}}\times\underline{\ddot{U}} + M^2_{ref}\underline{t}^0 \\ & + M^2_{ref}\frac{U_{ref}}{L}\underline{\dot{U}} + M^2_{ref}\frac{k_{ref}}{\Phi_0}\Omega\underline{t}^0 + M^2_{ref}\frac{k_{ref}}{\Phi_0}\frac{U_{ref}}{L}\Omega\underline{\dot{U}}.\end{aligned} \tag{A.31}$$

As before the quantities (U_{ref}/L) and (k_{ref}/Φ_0) are considered to be of order ε. Any term in (A.31) with two or more order ε terms will be neglected as being a higher order term. Only the last term is therefore neglected and the remaining terms are those shown in equation (3.70).

APPENDIX

B

Alternate Bases At End Of Segment

An important consideration in using the *segmental shooting technique* is to be able to determine a new orthonormal basis at the end of the current segment being solved. This new basis will then be used as the local basis in which to solve the next segment. There are several methods available to choose this new basis. This section considers some of the alternate choices available.

In determining the new basis at the end of the segment, the first item needed is the tangent direction. This can be obtained by the method outlined in Section 3.2.3. After the tangent direction, $\underline{e}_1$, has been determined, $\underline{e}_2$ and $\underline{e}_3$ which span the cross section must be determined. There are an infinite number of possible sets of ($\underline{e}_2$, $\underline{e}_3$) which satisfy this requirement. In Section 3.2.3, $\underline{e}_2$ and $\underline{e}_3$ were chosen to be the normal and binormal vectors of the Frenet basis. Other choices are possible, however. For example, rather than using a Frenet basis, a material basis could be used. A material basis is one in which the vectors are embedded in the material and deform along with the rod. Thus the orientation of this basis at the end of the segment is not arbitrary. It depends upon the orientation of the basis initially and also upon the deformation. Recall that the kinematically admissible variations in the vectors $\underline{e}_i^0$ are given from equation (2.34) as $\underline{v}_i(s) = \underline{a}(s) \times \underline{e}_i^0$, where $\underline{e}_i(s)=\underline{e}_i^0 + \underline{v}_i(s)$. The vector $\underline{a}(s)$ determines how a material basis $\{\underline{e}_i^0\}$ changes orientation along the rod segment.

To determine the vector $\underline{a}$, recall from equation (2.39) that $\underline{u}'=\underline{a}\times\underline{t}$. Then with $\underline{t}$ interpreted as $\underline{t}^0$ and with $\underline{u}$ given by equation (3.12), this gives the result that

$$a_2 = -\frac{dw}{ds} = -\epsilon, \qquad a_3 = \frac{dv}{ds} = \delta, \tag{B.1}$$

where the components of $\underline{a}$ are expressed in terms of the basis $\{\underline{e}_i^0\}$. To determine the a_1 component consider the case of a straight rod undergoing pure torsion. In such a case the tangent direction remains unchanged so that $\underline{v}_1=0$. This implies that a_2 and a_3 are zero. The vectors $\underline{e}_2(s)$ and $\underline{e}_3(s)$ change orientation by rotating around the axis of the rod. The amount of this rotation is equal to the total angle of twist of the rod segment,

γ, between arc length 0 and s. Thus a_1 at the end of the rod can be determined in several ways. One method is by integrating the twist per unit length of the rod, given in equations (3.17) and (3.52), between arc lengths ρ=0 and ρ=1, which gives

$$\gamma = \Phi_0 L + \frac{EI}{GJ}\left[\nu_{20}\sum_{k=0}^{\infty}\frac{\beta_k}{(k+1)(k+2)} - \chi_2\sum_{k=0}^{\infty}\frac{\beta_k}{(k+2)(k+3)}\right.$$
$$\left. - \nu_{30}\sum_{k=0}^{\infty}\frac{\alpha_k}{(k+1)(k+2)} + \chi_3\sum_{k=0}^{\infty}\frac{\alpha_k}{(k+2)(k+3)}\right] \qquad \text{(B.2)}$$
$$+ \frac{EI}{GJ}\int_0^{\rho}\left(\epsilon\frac{d\delta}{d\rho} - \delta\frac{d\epsilon}{d\rho}\right)d\rho\,.$$

Here the last term involves a nontrivial integration of two power series multiplied together which requires a significant computational effort. Also it was mentioned in Section 3.2.3 that γ as expressed in (B.2) does not represent the physical twist per unit length but is a representation of the change in M_1 in the original $\underline{e}_1^0$ direction and does not give an accurate indication of the actual total twist.

Another method is to assume that the exact result of twist per unit length along the rod being constant applies and that the total twist is simply ΦL. However the results of the exact solution may or may not be applicable to the approximate solution. Thus this approach may not be justifiable although the errors introduce would be small and would be expected to be negligible as the number of segments is increased.

With the vector $\underline{a}$ thus determined, the new material basis at the end of the segment can be determined. However, the basis obtained will not be exactly orthonormal. Each time a new vector is calculated, a small amount is added to the original unit vector. Thus the resulting "unit" vectors become slightly larger in

magnitude with each calculation and therefore do not remain unit vectors. The resulting vectors could be made unit vectors by normalizing them at the expense of increased computation. Further, the basis obtained in this manner will not be exactly orthonormal. There will be a slight deviation from orthonormality which could accumulate as the solution progresses. The basis could be orthonormalized, possibly using the Gram-Schmidt orthonormalization procedure for example, again at the further expense of increased computation.

Therefore the Frenet basis was chosen as being the best choice because it met all the requirements (orthonormality, $\underline{e}_1$ along the tangent direction) and was the simplest to compute. The instances when the Frenet basis is not uniquely defined (ie: rod remains straight) do not present any difficulty as mentioned in Section 3.2.3. This basis also has a further advantage in that the Frenet basis is used often in the literature and computing this basis at each segment may facilitate comparison with other problems and solutions.